UC Berkeley
UC Berkeley Previously Published Works

Title
Self-guarding of MORC3 enables virulence factor-triggered immunity

Permalink
https://escholarship.org/uc/item/9cm805hs

Journal
Nature, 600(7887)

ISSN
0028-0836

Authors
Gaidt, Moritz M
Morrow, Alyssa
Fairgrieve, Marian R
et al.

Publication Date
2021-12-02

DOI
10.1038/s41586-021-04054-5

Peer reviewed

Self-guarding of MORC3 enables virulence factor-triggered immunity

Moritz M. Gaidt[1,*], **Alyssa Morrow**[2], **Marian Fairgrieve**[1], **Jonathan Karr**[3], **Nir Yosef**[2,4], **Russell E. Vance**[1,5,6,*]

[1]Division of Immunology and Pathogenesis, Department of Molecular and Cell Biology, University of California, Berkeley, CA 94720 USA

[2]Electrical Engineering and Computer Science Department, University of California, Berkeley, CA 94720, USA

[3]Division of Genetics, Genomics and Development, Department of Molecular and Cell Biology, University of California, Berkeley, CA 94720 USA

[4]Center for Computational Biology, University of California, Berkeley, CA 94720 USA

[5]Cancer Research Laboratory and the Immunotherapeutics and Vaccine Research Initiative, University of California, Berkeley, CA 94720

[6]Howard Hughes Medical Institute, University of California, Berkeley, CA 94720

SUMMARY

Pathogens employ virulence factors to inhibit the immune system[1]. The guard hypothesis[2,3] postulates that hosts monitor (or 'guard') critical innate immune pathways such that their disruption by virulence factors provokes a secondary immune response[1]. Here, we describe a 'self-guarded' immune pathway in human monocytes, in which guarding and guarded functions are united in one protein. We find that this pathway is triggered by ICP0, a key virulence factor of Herpes Simplex Virus-1 (HSV-1), resulting in robust induction of anti-viral type I interferon (IFN). Surprisingly, induction of IFN by ICP0 is independent of canonical immune pathways and the IRF3/7 transcription factors. A CRISPR-screen identified the ICP0-target MORC3[4] as an essential negative regulator of IFN. Loss of *MORC3* recapitulates the IRF3/7-independent IFN response induced by ICP0. Mechanistically, ICP0 degrades MORC3, which leads to de-repression of a MORC3-regulated DNA element (MRE) adjacent to the *IFNB1* locus. The MRE is required *in cis* for *IFNB1* induction by the MORC3 pathway, but is not required for canonical IFN-inducing pathways. Besides repressing the MRE to regulate *IFNB1*, MORC3 is also a direct

restriction factor of HSV-1[5]. Our results thus suggest a model in which the primary anti-viral function of MORC3 is 'self-guarded' by its secondary IFN-repressing function: thus, a virus that degrades MORC3 to avoid its primary anti-viral function will unleash the secondary anti-viral IFN response.

The innate immune system employs germline-encoded pattern recognition receptors (PRRs) to sense conserved pathogen-associated molecular patterns (PAMPs) such as lipopolysaccharide and nucleic acids[6]. To exploit host cells, pathogens produce virulence factors that disrupt critical immune pathways[1]. As postulated by the guard hypothesis[3], immunity in plants relies on a secondary line of pathogen detection, which monitors (or 'guards') the integrity of host immune defense pathways. Virulence factor-mediated disruption of a guarded pathway triggers activation of a secondary immune response[1,2]. In mammals several guard-type immune pathways sense bacterial virulence factors[1], yet the overall importance of guard-immunity, especially during viral infections, is less clear.

Herpes Simplex Virus-1 (HSV-1) is a dsDNA-virus of the alphaherpesvirinae sub-family. Its DNA genome is recognized as a PAMP by the cyclic-GMP-AMP synthase (cGAS)– stimulator of interferon genes (STING) PRR-pathway[7]. Downstream of DNA recognition, STING[8] activates TANK Binding Kinase 1 (TBK1) and I-kappa-B kinase ε (IKKε) that phosphorylate and activate interferon regulatory factors 3 and 7 (IRF3/7), leading to transcriptional induction and secretion of type I interferon (IFN) cytokines[7]. IFNs bind to the IFNα/β receptor (IFNAR) to induce transcription of anti-viral interferon-stimulated genes (ISGs). HSV-1 replication is constrained by several intrinsic host defenses, including interferon gamma inducible protein 16 (IFI16) and nuclear domain 10 (ND10) nuclear bodies, also called promyelocytic leukemia protein (PML) nuclear bodies, which repress viral transcription[9,10]. If these defense mechanisms succeed, the virus is forced into latency. Consequently, HSV-1 employs the sumo-activated E3-ubiquitin-ligase infected cell protein 0 (ICP0)[9,11] to facilitate viral transcription and lytic replication by degrading or dispersing sumo-dependent IFI16 and ND10 nuclear bodies.

Innate sensing of viral virulence factors

To study the innate immune response to herpes viruses, we infected human BLaER1 monocytes[12] with HSV-1. Surprisingly, the induction of IFN as measured by transcription of *IFNB1* and the ISGs *RSAD2* and *CXCL10* was not solely dependent on STING, TBK1/IKKε or IRF3/7 (Fig. 1a, Extended Data Fig. 1a). In contrast, IFN induction in response to transfected dsDNA depended entirely on STING, TBK1/IKKε or IRF3/7, as expected.

ICP0 was necessary for HSV-1 to induce PRR-independent IFN in BLaER1 monocytes (Fig. 1b, Extended Data Fig. 1b). Induction of IFN by HSV-1 was abrogated only by deleting both the STING pathway from host cells and ICP0 from HSV-1 (Fig. 1b). The ICP0-triggered immune response did not require IKKα/IKKβ (Extended Data Fig. 1c, d) and was the main contributor to secreted IFNβ from infected BLaER1 monocytes (Extended Data Fig. 1e), presumably because it was activated as early as 3h after infection (Extended Data Fig. 1f). The redundancy between ICP0-triggered and STING-mediated immune activation was

confirmed in THP1 and U937 cells, two other human monocyte-like cell culture models (Extended Data Fig. 2).

ICP0 is critical for lytic replication of HSV-1[11] and consequently ΔICP0 HSV-1 was attenuated in BLaER1 monocytes (Extended Data Fig. 3). To address if ICP0 itself triggered PRR-independent IFN induction, we inducibly expressed ICP0 in human monocytes. Mirroring HSV-1 infection, ICP0 expression led to potent IFN induction (>10,000-fold) that was independent of TBK1/IKKε, IRF3/7 and IKKα/β (Fig. 1c, Extended Data Fig. 4a). Thus, ICP0 is sufficient for IFN induction. Ectopic expression of E4ORF3, a virulence factor from Adenovirus 5, whose loss can be functionally complemented by ICP0[13], induced a similarly potent IFN response independently of PRR signaling molecules (Fig. 1c, Extended Data Fig. 4a). These observations were confirmed in THP1 and U937 cells (Extended Data Fig. 4b, c). Consistent with its potent activity, ICP0 was hardly detected by immunoblot despite triggering a potent immune response (Extended Data Fig. 5a, b). An enzymatically inactive variant of ICP0[14] lacking the catalytic RING domain failed to induce IFN. The predominantly nuclear variant ICP0 D199A[15] was not impaired in IFN induction whereas the predominantly cytosolic ICP0 D8[14] variant was less potent (Extended Data Fig. 5a, b). RNAseq-analysis revealed induction of IFN and ISGs as the major consequence of viral virulence factor sensing (Extended Data Fig. 5c–f, Supplementary Table 1), which was comparable between ICP0- and E4ORF3-mediated immune activation. Thus, the immune system detects viral virulence factors including nuclear and catalytically active ICP0 from HSV-1.

Self-guarding of MORC3

We considered the hypothesis that ICP0 degrades a negative regulator of IFN, inadvertently triggering an IFN response (Fig. 2a). This hypothesis is consistent with the observation that perturbing the sumoylation machinery activates IFN[16,17]. We conducted a genome-wide CRISPR screen with the hope of identifying a nuclear, sumoylated substrate of ICP0 that negatively regulates IFN (Fig. 2b; Extended Data Fig. 6a,b; Supplementary Table 2). The screen utilized Viperin levels to report the IFN-status via autocrine signaling at single cell resolution (Extended Data Fig. 6a). Several individual sgRNAs were validated to enhance Viperin expression at steady state with varying effect sizes (Fig. 2b), including sgRNAs targeting *TRIM33* and *USP18*, known negative regulators of PRR-mediated IFN induction and IFNAR signaling[18,19]. In addition, sgRNAs targeting the sumoylated nuclear body protein *MORC3* induced Viperin expression. Consistent with these observations, mice heterozygous for a *Morc3* mutation were reported to exhibit bone and hematopoietic abnormalities and elevated interferon expression[20], although the pathway leading to IFN induction was not elucidated. We decided to focus on MORC3 as it was previously described to be degraded by ICP0 in fibroblasts[4,5]. We confirmed that ICP0 was required for MORC3 degradation during HSV-1 infection in BLaER1 monocytes (Fig. 2c) and U2OS cells, which support ICP0-independent HSV-1 replication (Extended Data Fig. 6c). MORC3 degradation occurred as early as 3h after infection (Fig. 2d) at the same timepoint when STING-independent IFN is being made (Extended Data Fig. 1f). Independently generated *MORC3*^{−/−} BLaER1 monocytes (Fig. 2e, f, Extended Data Fig. 6d–i), or *MORC3*-targeted THP1 (Extended Data Fig. 7a, b) and U937 (Extended Data Fig. 7c, d) myeloid-like cells

displayed spontaneous (up to 10,000-fold) IFN induction and IFNAR-dependent responses (Extended Data Fig. 6i). Similar to ICP0-mediated IFN, the response of *MORC3*^{−/−} BLaER1 cells was independent of PRR-signaling hubs TBK1/IKKε, IRF3/7 and IKKα/β (Fig. 2e, f, Extended Data Fig. 6d–i). Global transcriptomic changes in *MORC3*^{−/−} monocytes were dominated by ISG induction and recapitulated the transcriptional changes induced by virulence factors (Fig. 2g; Extended Data Fig. 7e, f; Supplementary Table 1). These results identify the ICP0-target MORC3 as a negative regulator of IFN in human monocytes.

MORC3 is a member of the MORC-gene family of GHKL (gyrase, Hsp90, histidine kinase, MutL)-type ATPases that are transcriptional repressors[21,22]. It co-localizes with PML/ND10 nuclear bodies[23]. PML is also degraded by ICP0[9], yet there was no role for PML in the MORC3 pathway of IFN induction (Extended Data Fig. 8a–c). Thus, IFN regulation is a specific function of MORC3 and not of PML/ND10 nuclear bodies. Localization of MORC3 to anti-viral ND10 nuclear bodies suggests a role for MORC3 during viral infection. Whereas one report observed enhanced viral replication in MORC3 knockdown cells (implying an anti-viral function of MORC3)[5], other studies reported diminished viral replication in MORC3 knockdown cells[24] and increased viral replication upon MORC3 overexpression[25] (implying a pro-viral function of MORC3). We suggest that MORC3 has two functions: (1) a primary function to repress viral replication; and (2) a secondary function to repress IFN/ISG induction. The primary function of MORC3 is apparent in cells that do not induce IFN upon MORC3 loss, such as HCT116 cells (Extended Data Fig. 8d, e), or do not respond to IFN, such as IFNAR-deficient BLaER1 monocytes. In these cells, loss of MORC3 results in enhanced replication of ΔICP0 HSV-1 (Fig. 3a, Extended Data Fig. 8f). WT HSV-1 employs ICP0 to degrade MORC3 to alleviate this restriction. Consequently, only ΔICP0 HSV-1 benefits from the deletion of *MORC3* (Fig. 3a)[5]. In IFNAR-sufficient monocytic cells, loss of *MORC3* results in IFN induction and viral restriction. Restriction is due to elevated IFN in the absence of *MORC3* because viral gene expression was fully restored in *MORC3*^{−/−}*IFNAR1*^{−/−}*IFNAR2*^{−/−} cells (Fig. 3b). We thus propose that the primary anti-viral function of MORC3 is guarded by its secondary IFN-repressing function (Fig. 3c). Combining both guarded and guarding function in one protein generates the molecular equivalent of a dead-man's switch—a self-monitoring, self-insured anti-viral immune pathway.

Location-dependent de-repression of *IFNB1*

MORC3 deficiency is associated with de-repression of endogenous retroviruses (ERVs) in embryonic stem (ES) cells[26] and ERV de-repression can cause IFN induction[27]. However, we observed only minor effects on ERV expression in *MORC3*^{−/−} BLaER1 cells (Extended Data Fig. 9), suggesting a different regulatory function for MORC3 in monocytes versus ES cells and that the IFN de-repression in *MORC3*^{−/−} monocytes is not caused by ERVs. Next, we found that the majority of transcriptional changes incurred by *MORC3* deficiency were due to IFNAR signaling (Extended Data Fig. 10a, b). The most significantly de-repressed genes in *MORC3*^{−/−}*IFNAR1*^{−/−}*IFNAR2*^{−/−} monocytes are *MLLT3*, *IFNB1* and *FOCAD*, which, remarkably, are clustered together within a short section of chromosome 9 (chr9:20,329,000–21,086,000; Fig. 3d). Adjacent genes in both directions were not

MORC3-regulated (Extended Data Fig. 10c). Transcriptional up-regulation of *MLLT3* was not a general feature of antiviral immune activation because PRRs did not induce *MLLT3* transcription (Extended Data Fig. 10d). We hypothesized that MORC3 acts in a locus-specific manner to regulate gene expression.

Interestingly, *IFNB1* is the only *IFN* gene that is de-repressed in *MORC3*^{−/−} cells (Extended Data Fig. 10c, e). While IFN genes other than *IFNB1* can mediate ISG induction in response to foreign DNA (Fig. 3e, Extended Data Fig. 10f, g) *IFNB1* is required to activate ISGs in the absence of *MORC3* (Fig. 3f, Extended Data Fig. 10a, h–j). HSV-1 infection led to upregulation of the gene cluster on chromosome 9, as judged by *MLLT3* expression, in an ICP0-dependent manner (Extended Data Fig. 11a). Ectopic expression of ICP0 or E4ORF3 resulted in the locus-specific induction of *IFNB1* and its neighboring genes (Extended Data Fig. 11b), only de-repressed *IFNB1* of all *IFN* genes (Extended Data Fig. 11c), and required *IFNB1* for induction of ISGs (Extended Data Fig. 11d–f). As expected, the resistance of *MORC3*^{−/−} cells to viral infection required *IFNB1* (Fig. 3g). We conclude that MORC3 acts selectively on the *IFNB1* locus. Thus, in contrast to STING-signaling, anti-viral ISG induction by the MORC3 pathway uniquely relies on *IFNB1*.

A MORC3-regulated element activates IFNB1

Consistent with the locus-specific gene regulation by MORC3, a randomly integrated *IFNB1*-promoter-luciferase reporter was only induced by DNA-STING signaling but not by *MORC3* deficiency (Extended Data Fig. 12a). As expected, the endogenous *IFNB1* gene was activated both by STING signaling and *MORC3* deficiency (Extended Data Fig. 12b). Thus, a functional element outside the promoter is required for *IFNB1* expression in the absence of MORC3. ATAC-seq identified a minisatellite-like element[28] that we call the MORC3-regulated element (MRE) in an intron of *FOCAD*, approximately 100kb downstream of *IFNB1*, that gains DNA accessibility in the absence of *MORC3* (Fig. 4a, b). The MRE was required for *IFNB1* and *MLLT3* de-repression in *MORC3*^{−/−} cells but not for *IFNB1* induction upon PRR signaling, indicating that the MRE is a specific component of the MORC3 pathway (Fig. 4c, Extended Data Fig. 12c, d). Although the MRE is located in an intron of *FOCAD*, FOCAD protein expression was not impaired in MRE^{−/−} cells, and neither *FOCAD* nor *MLLT3* were required for *IFNB1* induction in absence of *MORC3* (Extended Data Fig. 12e–g). We find that the MRE regulates *IFNB1* in *cis* because a MORC3-sgRNA drove bi-allelic expression of *IFNB1* in WT cells and mono-allelic expression of *IFNB1* in heterozygous MRE^{+/−} cells (Fig. 4d, e). Confirming the regulation in *cis*, only chromosome-9-located high-confidence *MORC3*-repressed genes (identified in all RNA-seq conditions) required the MRE to be induced in absence of *MORC3* (Fig. 4f). The effect size of de-repression of genes outside of the chromosome 9 locus is minor (Extended Data Fig. 12h), indicating that the regulation of *IFNB1* and surrounding genes is the main effect of the MORC3 pathway in monocytes. The MRE was required for ICP0/E4ORF3-induced *IFNB1* and *MLLT3* transcription (Fig. 4g, h) as well as for ICP0-dependent *IFNB1* induction during HSV-1 infection (Fig. 4i). As ΔICP0 HSV-1 is attenuated, we used a 25× higher MOI leading to comparable ICP4 expression between WT and ΔICP0 HSV-1 (Extended Data Fig. 12i). MORC3 was still degraded by ICP0 in absence of the MRE, confirming that MORC3 degradation is upstream of MRE activation

(Extended Data Fig. 12i). Lastly, to confirm key aspects of the MORC3 pathway in primary immune cells, we targeted *MORC3* in primary human macrophages and observed a strong, spontaneous upregulation of *IFNB1*, *MLLT3*, and ISGs (Extended Data Figure 12j).

Our results identify the MORC3-pathway as a novel innate immune sensing pathway that detects the activity of virulence factors from DNA viruses, such as ICP0 from HSV-1 (Fig. 4j). The self-guarded protein MORC3 inhibits replication of HSV-1. To escape restriction, HSV-1 employs ICP0 to degrade MORC3. MORC3's secondary function to repress the MORC3-regulated DNA element (MRE), adjacent to the *IFNB1* locus, allows induction of IFN upon viral attack on MORC3. The integration of two distinct functions within a single 'dead-man's switch' provides robust self-insurance of the anti-viral MORC3 function. Employing a single protein to repress both viral gene expression and antiviral IFN may be a general strategy against viruses (see Supplementary Note).

Material and Methods

Cell culture

BLaER1, U937 and THP-1 cells were cultured in RPMI Medium 1640 supplemented with L-glutamine, sodium pyruvate, 100U/ml penicillin-streptomycin (Thermo Fisher) and 10% (v/v) FCS (Omega Scientific). HEK293T, U2OS and HCT116 cells were cultivated in DMEM Medium (Thermo Fisher) containing the same supplements. Human macrophages were cultivated in DMEM with similar supplements and recombinant 100 ng/ml M-CSF (Peprotech). 1.4 million BLaER1 cells per well of a 6-well plate were trans-differentiated into monocytes for 5–6 days in medium containing 10 ng/ml of hrIL-3, 10 ng/ml hr-CSF-1 (M-CSF) (both PeproTech) and 100 nM β-Estradiol (Sigma-Aldrich) as previously described[29,30]. 1.4 million THP-1 and U937 cells per well of a 6-well plate were differentiated overnight with 100 ng/ml PMA (Sigma-Aldrich). STING-deficient and corresponding control THP1 and U937 cells were a gift from Dan Stetson (University of Washington). BLaER1 cells were a gift from Thomas Graf (CRG, Barcelona, Spain) and Veit Hornung (LMU Munich, Germany). U2OS cells were a gift from Robert Tjian and Xavier Darzacq (UC Berkeley). THP1 cells were from ATCC. U937 cells were from the UC Berkeley Cell Culture Facility. HCT116 cells were a gift from David Raulet (UC Berkeley).

Cell stimulation

For activation of the PRR-pathways, 3.2μg of UltraPure™ Salmon Sperm DNA (Thermo Fisher), 3.2μg of 2'3' cGAMP (Invivogen) or 3.2μg 3P-RNA (Invivogen) was complexed with 8μl Lipofectamine 2000 (Thermo Fisher) according to the manufacturer's protocol in Opti-MEM Reduced Serum Media (Thermo Fisher) and added to 1.4 million cells per well of a 6-well plate for 3h or the indicated time. TLRs were activated with 200 ng/ml LPS-EB ultrapure from *E. coli* O111:B4 (Invivogen) or 500ng/ml R848 (Invivogen). For activation of doxycycline-inducible trans-gene expression, cells were stimulated with 1μg/ml doxycycline hyclate (Sigma-Aldrich) for 24h.

HSV-1 infection

BACs of F-strain ICP0 HSV-1 and corresponding F-WT strain were a gift from Bernard Roizman (University of Chicago). BAC DNA was prepared from a mono-clonal transformant, sequence verified by deep sequencing and transfected into U2OS cells using Lipofectamine 2000 (Thermo Fisher). Virus was propagated, harvested and frozen as described[31]. Viral progeny were titered from cell-free supernatants by TCID50 using 8 replicates per dilution. U2OS cells were used for titering if not otherwise indicated, and FFU/ml was calculated by the Spearman & Kärber algorithm. Myeloid cells were infected by adsorbing virus of appropriate MOI in FCS free RPMI Medium 1640 for 1h. For analysis of viral progeny in the supernatant, cells were subsequently washed 3 times with warm PBS and resuspended in RPMI. For all other experiments, medium was directly changed to RPMI without PBS wash.

Quantification of gene expression

Gene expression was quantified by RT-qPCR. RNA was isolated with E.Z.N.A. Total RNA kit I (Omegabiotek) and 0.5–1μg RNA was treated with RQ1 RNase-free DNase (Promega) in presence of RNasin plus Ribonuclease Inhibitor (Promega). RNA was reverse transcribed with Superscript III reverse transcriptase (Invitrogen). SYBRGreen dye (Thermo Fisher Scientific) was used for quantitative PCR assays and analyzed with a real-time PCR system (StepOnePlus; Applied Biosystems). All gene expression values were normalized to GAPDH and are depicted as $2^{-\Delta Ct}$ ($Ct_{target} - Ct_{GAPDH}$)

RSAD2.fwd	CAACTACAAATGCGGCTTCT
RSAD2.rev	ATCTTCTCCATACCAGCTTCC
CXCL10.fwd	TCTGAATCCAGAATCGAAGG
CXCL10.rev	CTCTGTGTGGTCCATCCTTG
GAPDH.fwd	GAGTCAACGGATTTGGTCGT
GAPDH.rev	GACAAGCTTCCCGTTCTCAG
IFNB1.fwd	CAGCATCTGCTGGTTGAAGA
IFNB1.rev	CATTACCTGAAGGCCAAGGA
MLLT3.fwd	GAGCACAGTAACATACAGCA
MLLT3.rev	GGCAAAATGAAACCAGCATA

Immunoblotting

Whole cell lysates were prepared by lysing cells in 50mM Tris pH7.4, 50mM NaCl, 2mM MgCl$_2$, 0.5% NP40, 25U/ml Benzonase® Nuclease (Millipore Sigma) and Complete Mini EDTA-free Protease Inhibitor (Roche) for 20 min on ice. Laemmli buffer was added to a final concentration of $1\times$ and lysates were boiled at 95°C for 10 minutes. Proteins were separated with denaturing PAGE and transferred to Immobilon-FL PVDF membranes (Millipore Sigma). Membranes were blocked with Li-Cor Odyssey blocking buffer. Primary antibodies were added and immunoblots incubated overnight. Antibodies used were anti-β-Actin (C4) (Santa Cruz, sc-47778, 1:2000), anti-HSV-1 ICP4 (H943) (Santa Cruz, sc-69809, 1:200), anti-HSV-1 ICP0 (11060) (Santa Cruz, sc-53070, 1:200), anti-TBK1 (D1B4) (Cell

Signaling, #3504, 1:1000), anti-IKKε (Cell Signaling, #2690, 1:1000), anti-IRF-3 (D83B9) (Cell Signaling, #4302, 1:1000), anti-IRF-7 (Cell Signaling, #4920, 1:1000), anti-IKKβ (2C8) (Cell Signaling, #2370, 1:1000), anti-IKKα (3G12) (Cell Signaling, #11930, 1:1000), anti-MORC3 (NovusBio, NBP1-83036, 1:500), anti-MORC3 (Proteintech, 24994-1-AP, 1:500), anti-FOCAD (NovusBio, NBP2-49163, 1:1000), anti-MLLT3 (AF9 polyclonal antibody, Invitrogen, PA5-81972, 1:250), anti-PML (Bethyl Laboratories, A301-167A-M, 1:1000). Appropriate secondary IRDye®-conjugated antibodies (Li-Cor) were used and immunoblots were imaged using the Li-Cor Odyssey platform. See Supplementary Fig. 2–4 for raw, uncropped images.

Quantification of allele-specific IFNB1 expression

To ask if the MRE regulates *IFNB1* in *cis* or in *trans*, we engineered the *IFNB1* coding sequence with distinct indels. This allowed us to track which allele is being transcribed upon activation of *IFNB1* by amplicon sequencing of *IFNB1* cDNA (Fig. 4d). Cytosolic DNA sensing drove bi-allelic activation of *IFNB1* regardless of the MRE (Fig. 4e). Activating the MORC3 pathway with a MORC3-sgRNA drove bi-allelic expression in WT cells and mono-allelic expression of *IFNB1* in heterozygous MRE$^{+/}$ cells (Fig. 4e). While the long distance between *IFNB1* and the MRE makes it difficult to determine which indel-marked *IFNB1* allele is in *cis* with MRE , these data strongly suggest that the MRE induces *IFNB1* transcription in *cis*. Specifically, the genome of heterozygous MRE$^{+/}$ and corresponding WT (*STAT1*$^{-/-}$*STAT2*$^{-/-}$ Cas9) BLaER1 cells was edited at the IFNB1 locus using the sgRNA GATGAACTTTGACATCCCTG**AGG** as described in "CRISPR/Cas9 mediated gene targeting". Monoclonal lines harboring to different indels were subcloned. Cells were transduced with scramble or *MORC3*-targeting sgRNA. Oligo-dT-cDNA from trans-differentiated BLaER1 was prepared. The indel containing sequence was amplified from the cDNA using the primers:.

IFNB1_fwd	ACACTCTTTCCCTACACGACGctcttccgatctCCATGAGCTACAACTTGCTTGGA
IFNB1_rev	TGACTGGAGTTCAGACGTGTGctcttccgatctAGCCAGGAGGTTCTCAACAATAG

Illumina handles and barcodes were added as previously described[32] and sequenced on an Illumina Miseq 250SR V2. Data was analyzed using Outknocker[33].

CRISPR/Cas9 mediated gene targeting

Monoclonal gene-deficient BLaER1 cells were generated as follows. Briefly, sgRNAs specific for the indicated genes were designed to target an early coding exon of the respective gene with minimal off-targets and high on-target activity using ChopChop[34]. U6-sgRNA-CMV-mCherry-T2A-Cas9 plasmids were generated by ligation-independent-cloning as previously described[35] and BlaER1 cells were electroporated using a Biorad GenePulser device. Automated cell sorting was used to collect mCherry positive cells that were cloned by limiting dilution. Monoclonal cell lines were identified, rearranged and duplicated for genotyping using deep sequencing as previously described[32]. Knockout cell clones contained all-allelic frame shift mutations without any wild type reads. The MRE

was deleted using indicated sgRNAs below to induce a ~3kb deletion. Two independent knockout single-cell clones were analyzed per genotype, and one representative clone per genotype is shown. For polyclonal gene targeting, cell lines were transduced with lentiCas9-Blast[36], a gift from Feng Zhang (Addgene plasmid #52962). sgRNAs were designed as above and cloned into lentiGuide-Puro[36], a gift from Feng Zhang (Addgene plasmid # 52963), using ligation-independent-cloning. Cas9-expressing cells were transduced with indicated sgRNA-encoding lenti-viruses. Gene deficient clones were independently validated either by loss of function or by loss of protein expression.

sgRNA target sites (PAM is highlighted in bold):

STING1	GCGGGCCGACCGCATTTGGG**AGG**
TBK1	ACAGTGTATAAACTCCCACA**TGG**
IKBKE (IKKε)	TGCATCGCGACATCAAGCCG**GGG**
CHUK (IKKα)	TAGTTTAGTAGTAGAACCCA**TGG**
IKBKB (IKKβ)	GCCATGGAGTACTGCCAAGG**AGG**
IRF7	CCGAGCTGCACGTTCCTATA**CGG**
IRF3	GTTACTGGGTAACATGGTGT**TGG**
TRIM33	GTTATGAACTTCACAAATT**GGG**
VMP1	GAACTGCCAGTTTGGCCC**GGG**
UBA3	GGCCTAAGGAGCAGCCTTT**TGG**
NAE1	GAATTAAATAGCGATGTCTC**TGG**
NF1	GCTGGTTTCCTTCACGAC**AGG**
USP18	GGCACAGTCAACGCAAATCA**AGG**
NFIC	GCTGCTGGGCGAGAAGCCCG**AGG**
EFR3A	GATTGCTATGGAGGCAC**TGG**
PTPN1	GAGCAGATCGACAAGTCC**GGG**
MORC3	GCTGATACTGAGATACCATA**TGG**
TAF5L	GCTGCTCAATGACATCCTTC**TGG**
RNF7	GGCCATGTGGAGCTGGGACG**TGG**
PI4KA	GGGATAGCATACTTGCAA**AGG**
IFNAR1	GTACATTGTATAAAGACCAC**AGG**
IFNAR2	TGAGTGGAGAAGCACACACG**AGG**
STAT1	CAGGAGGTCATGAAAACGGA**TGG**
STAT2	ATCATCTCAGCCAACTGGGT**AGG**
IFNB1	GATGAACTTTGACATCCCTG**AGG**
FOCAD	AGAGGCGATGATGTTTATTG**AGG**
MLLT3	GTACGAACACCATCCAGTCG**TGG**
PML_1[*]	AGACCTCACTTCCTATGACG**GGG**
PML_2[*]	AGTGCTTCGAGGCACACCAG**TGG**
MRE_1	AACCCTAATGTACACTTGGT**AGG**
MRE_2	CACTTCTAGAACGGTCACCA**TGG**
scramble	GCTGCTCCCTAACAGGACGC

*PML KO have all allelic frame shift mutations at both sgRNA target sites

Cytokine quantification

Cytokine secretion was quantified by ELISA of cell-free supernatants after stimulation (IFNβ: R&D, DY814-05; IP-10: BD, 550926).

Lenti-/retro-viral transduction

Lenti- and retro-virus was produced in HEK293T cells. 4.5 million cells were plated per 10cm dish and transfected with 5μg of transfer vector, 3.75μg of packaging vector (pd8.9 for lenti- and pGAGPOL for retro-virus) and 1.5μg pVSVG using 30.75μg PEI-MAX (Polysciences, 24765-1). 12h after transfection the medium was replaced with DMEM medium containing 30% (v/v) FCS. After 24h-36h, viral supernatants were harvested, centrifuged at $1000 \times g$ for 10min, and filtered through a 0.45μm filter. Cells were cultured for 48 after transduction, prior to selection with puromycin or Blasticidine S hydrochloride (both Sigma-Aldrich).

Ectopic gene expression

A doxycycline-inducible lentivirus system was used for ectopic gene expression. It uses a derivate of the plasmid pLIX_402 (Addgene #41394) that was adapted for restriction enzyme-based cloning by removing the attR1-ccdB-attR2 sites as previously described[30]. Codon-optimized constructs for HSV-1-ICP0 and HA-Adenovirus5-E4ORF3 were synthesized by Integrated DNA Technologies and cloned into pLIP. ICP0 variants were generated by overlap-extension PCR.

IFNB1-reporter

The 1kb upstream of the transcription start site of human *IFNB1* (hg38 chr9:21077923–21078922) was synthesized by Integrated DNA Technologies and cloned in front of a luciferase reporter from *Gaussia princeps*[37] into a retro-viral transfer vector in opposite direction to the 5′LTR. BLaER1 cells were transduced and sorted for reporter integration.

Flow Cytometry

For analysis of viperin expression BLaER1 were harvested for flow cytometry, fixed and permeabilized using eBioscience™ IC Fixation Buffer and eBioscience™ Permeabilization Buffer (both Thermo Fisher) according to the provider's protocol. Cells were incubated for 1h with PE-Anti-Viperin (Clone MaP.VIP; BD, 565196) at 4 μg/ml, washed 3 times and analyzed using a BD LSRFortessa™ Flow Cytometer. If indicated, cells were sorted on a BD FACSAria™ Fusion Cell Sorter. For analysis of HSV-1 infection BLaER1 were harvested for flow cytometry, fixed in 4% PFA (Electron Microscopy Sciences) for 15 min at room temperature and washed 3 times with PBS. Cells were permeabilized with HSV-1 stain buffer (PBS, 10% FCS, 1 mM EDTA and 0.1% Saponin) for 30 min on ice, incubated with Human BD Fc Block (BD) for 30 min on ice and stained with anti-HSV-1 antibody (ab9533, Abcam) at 1:100 dilution for 1 h on ice. After 3 washes with HSV-1 staining buffer, cells were stained with anti-rabbit secondary antibody (A-21244, Thermo Fisher Scientific) at 1:2000 dilution in HSV-1 stain buffer, washed 4 times in HSV-1 stain buffer and analyzed

using a BD LSRFortessa™ Flow Cytometer. See Supplementary Fig. 1 for representative gating strategies.

CRISPR-Screen

Monoclonal Cas9-expressing BLaER1 cells were re-selected with blasticidine and 9 million cells were transduced in four biological replicates with a pooled Human CRISPR Knockout library at an MOI of approximately 0.3. The library was a gift from Michael Bassik (Addgene #101926, 101927, 101928, 101929, 101930, 101931, 101932, 101933, 101934). Two days after transduction, cells were selected with puromycin for 3 days and trans-differentiated. Cells were stained for Viperin expression. Per biological replicate, 46–80 × 10^3 cells with increased spontaneous Viperin expression were sorted into direct lysis buffer (0.2 mg/ml proteinase K, 1 mM CaCl2, 3 mM MgCl2, 1 mM EDTA, 1% Triton × 100, 10 mM Tris pH 7.5). See Supplementary Fig. 1 for representative gating strategies. As control, sgRNA positive cells were sorted irrespectively of their Viperin expression. The reactions were incubated at 65 °C for 10 min and at 95 °C for 15 min. The integrated sgRNA cassette was amplified using a nested PCR approach with Phusion DNA Polymerase (Thermo Fisher) with 4 technical replicates per biological replicate. Primers for the first level utilized a mix of staggered forward primers:

pMCB320fwd 0nt stagger	ACACTCTTTCCCTACACGACGCTCTTCCGATCTCCTTGGAGAACCACCTTGTTGG
pMCB320fwd 1nt stagger	ACACTCTTTCCCTACACGACGCTCTTCCGATCTCCCTTGGAGAACCACCTTGTTGG
pMCB320fwd 2nt stagger	ACACTCTTTCCCTACACGACGCTCTTCCGATCTGCCCTTGGAGAACCACCTTGTTGG
pMCB320fwd 3nt stagger	ACACTCTTTCCCTACACGACGCTCTTCCGATCTAGCCCTTGGAGAACCACCTTGTTGG
pMCB320fwd 4nt stagger	ACACTCTTTCCCTACACGACGCTCTTCCGATCTCAACCCTTGGAGAACCACCTTGTTGG
pMCB320fwd 6nt stagger	ACACTCTTTCCCTACACGACGCTCTTCCGATCTTGCACCCCTTGGAGAACCACCTTGTTGG
pMCB320fwd 7nt stagger	ACACTCTTTCCCTACACGACGCTCTTCCGATCTACGCAACCCTTGGAGAACCACCTTGTTGG
pMCB320fwd 8nt stagger	ACACTCTTTCCCTACACGACGCTCTTCCGATCTGAAGACCCCCTTGGAGAACCACCTTGTTGG
pMCB320rev2	TGACTGGAGTTCAGACGTGTGCTCTTCCGATCTTCACCACACACGGCACTTACCT

Details of the nested PCR approach and primers for the second level PCR have been described[32]. PCR products were sequenced on Illumina HiSeq4000 50SR. Deep sequencing data was analyzed with PinAPL-Py[38]. The recovery of the sgRNA library was suboptimal, probably due to low number of sorted cells. Subsequently, reads from all technical and biological replicates were combined and enriched sgRNAs over control were identified. Modified robust ranking aggregation (RRA) to gene level revealed candidate negative regulators of IFN (Supplementary Table 2). Candidates with a significantly highly ranked sgRNAs (p.adjust <0.01) were validated in an arrayed format (Fig. 2c).

RNA-Seq

RNA from 2.8 million trans-differentiated BLaER1 monocytes was isolated using TRIzol™ Reagent (Thermo Fisher) according to the manufacturer's recommendation. DNA was removed with RQ1 RNase-free DNase (Promega) in the presence of RNasin plus Ribonuclease Inhibitor (Promega) and RNA isolated with Agencourt AMPure XP beads (Beckman Coulter). mRNA-seq libraries were prepared by the QB3 Genomics Functional Genomics Laboratory from poly-A-enriched mRNA using a KAPA mRNA HyperPrep Kit (Roche) and sequenced on the Illumina Novaseq S4 150PE. Sequencing quality of fastq files was evaluated with FASTQC version 0.11.5[39] and paired end RNA-seq reads were aligned to the reference genome (GRCh38.83) using Bowtie2 version 2.3.2[40] with default settings. Transcript and gene counts were quantified using RSEM[41] with the parameter 'strandedness' set to 'reverse' to account for strand-specific library preparation protocol. DeSeq2 version 1.30.1[42] was used to identify differentially expressed genes between conditions by building a single DeSeq2 model using counts from RSEM and performed pairwise comparisons of conditions. We consider all genes with a false discovery rate (FDR) below 0.05 to be significantly differential. We used log normalized counts from DeSeq2 to perform principal component analysis (PCA) shown in Figure 2 and to generate heatmaps. Gene enrichment analysis was done with the R package clusterProfiler version 3.18.1[43]. For each enrichment analysis, we assign the foreground to be the set of genes with significant increased expression in the condition being evaluated. We then set the background to the set of all genes that have mean counts greater than 1 for the condition being evaluated. Gene enrichment sets were downloaded using the R package msigdbr version 7.2.1. from the Molecular Signatures Database (MSigDB)[44].

ATAC-Seq

ATAC-seq was performed as previously described[45]. 50,000 BLaER1 monocytes were washed with PBS and lysed in 50 μL of cold lysis buffer (10 mM Tris-HCl, pH 7.4, 10 mM NaCl, 3 mM MgCl2, 0.1% IGEPAL CA-630). Nuclei were harvested by centrifugation and resuspended in 50 μl TD Buffer (Illumina, FC-121-1030) with 2.5 μL Tn5 Transposase (Illumina, FC-121-1030). The reaction was incubated for 30 min at 37°C and DNA was isolated with a MinElute Kit (Qiagen). Transposed DNA fragments were amplified to reach 30% of maximal amplification using Ad1 and Ad2 primer and sequenced on an Illumina Nova-Seq SP 50PE.

Ad1:	AATGATACGGCGACCACCGAGATCTACACTCGTCGGCAGCGTCAGATGTG
Ad2.1	CAAGCAGAAGACGGCATACGAGATTCGCCTTAGTCTCGTGGGCTCGGAGATGT
Ad2.2	CAAGCAGAAGACGGCATACGAGATCTAGTACGGTCTCGTGGGCTCGGAGATGT
Ad2.3	CAAGCAGAAGACGGCATACGAGATTTCTGCCTGTCTCGTGGGCTCGGAGATGT
Ad2.4	CAAGCAGAAGACGGCATACGAGATGCTCAGGAGTCTCGTGGGCTCGGAGATGT
Ad2.5	CAAGCAGAAGACGGCATACGAGATAGGAGTCCGTCTCGTGGGCTCGGAGATGT
Ad2.6	CAAGCAGAAGACGGCATACGAGATCATGCCTAGTCTCGTGGGCTCGGAGATGT

FASTQC version 0.11.5[39] was used to assess quality of ATAC-seq reads. Adaptor sequences were removed using Cutadapt version 2.10[46] using a default error rate of 0.1. Reads shorter

than 5 were discarded. Reads were aligned to the hg19 reference genome using bowtie 2 version 2.3.2[40] and discordant alignments were removed. Reads with mapping quality less than 30 were removed using SAMtools version 1.3.1[47] and duplicates were removed using Picard Tools version 2.5.0[48]. Additionally, regions overlapping black list regions, identified from the ENCODE consortium[49], were removed. Blacklist regions were downloaded from ENCODE (accession ENCFF000KJP). ATAC-seq reads aligned to the positive strand were shifted +4bp and reads aligned to the negative strand were shifted -5bp to adjust read start sites to represent the center of the transposase binding event[50]. Peaks were called on shifted reads using MACS2 version 2.2.7.1[51], setting the FDR to 0.05 and the default human genome size. Peaks from all samples were combined by taking the union of all peaks. Counts representing peak strength for all samples were obtained by counting the number of cut sites that overlapped each peak for each sample. DeSeq2 version 1.30.1[42] was used to identify the differential abundance of cut sites between conditions. All regions with an FDR below 0.05 were marked as significantly differentially accessible. Annotatr[52] was used to gather annotations of ATAC-seq peaks from the hg19 genome. To identify peaks that did not overlap promoters, all ATAC-seq peaks that overlapped at least one annotated promoter were removed.

Quantification of expression of ERV families

RNA-seq reads from $IFNAR1^{-/-}IFNAR2^{-/-}$ mCherry and $MORC3^{-/-}$ $IFNAR1^{-/-}IFNAR2^{-/-}$ BLaER1 monocytes were aligned to the hg38 genome using the STAR aligner 2.5.3a[53] with parameter 'outFilterMultimapNmax' set to '100000000' to allow for lenient alignment of multimapped reads. RepEnrich2[54] was used to quantify expression of ERV families. The MAPQ threshold for subsetting uniquely mapping and multi-mapping reads in RepEnrich2 was set to 255. We use pre-built repeat annotations for RepEnrich2, available through the RepEnrich2 GitHub[55]. We analyzed differential expression of ERV counts from RepEnrich2 using both the recommended edgeR version 3.32.1[56] and DeSeq2 version 1.30.1[42] pipelines to identify an overlapping set of high confidence differentially expressed ERVs. All ERVs with an FDR below 0.05 were considered to be significantly differential.

Statistical analysis

Data was analyzed for statistically significant differences using GraphPad Prism 8. Gene expression values were log2 transformed and viral titers were log10 transformed for statistical analysis. Statistical tests are indicated in the figure legends and were RM one-way or two-way ANOVA and Dunnett's or Bonferroni's post hoc test or paired, two-sided T-test. In case of two-way ANOVA the factors were genotype and stimulus. Normality and sphericity of data was assumed and not tested. * $p < 0.05$; ** $p < 0.01$ *** $p < 0.001$.

Gene targeting in primary human macrophages

Human peripheral blood mononuclear cells (PBMCs) from de-identified donors were obtained from AllCells (Alameda, CA, USA) under donor-informed consent and Alpha IRB approval obtained by AllCells (7000-SOP-045) for the study "Non-Mobilized Mononuclear Cell Apheresis Collection from Healthy Donors for the Research Market". Monocytes were isolated by negative selection (Pan Monocyte Isolation Kit, Miltenyi Biotec) and

nucleofected with Cas9:gRNA ribonucleoparticles as previously described[57]. Alt-R crRNAs and Alt-tracrRNA (IDT) were resuspended to 100 μM in nuclease-free duplex buffer (IDT) and annealed at equimolar concentrations for 5 min at 95°C and 15 min at 20°C. 10 μg Cas9 (IDT Alt-R S.p. Cas9 Nuclease V3) was mixed with 2 μl of the crRNA:tracrRNA complex and incubated for 20 min at room temperature before 1 μl of a 4 μM solution of electroporation enhancer (IDT) in nuclease-free duplex buffer (IDT) was added. 1e6 monocytes in 20 μl P3 nucleofection solution (Lonza) were added to the Cas9:crRNA:tracrRNA complex and nucleofected with a Lonza 4D-Nucleofector (4D-Nucleofector Core Unit, 4D-Nucleofector X Unit) using the settings Buffer P3, CM-137. Cells were immediately resuspended in pre-warmed medium and cultivated for 5 days. Every other day half of the medium was replaced with fresh medium.

crRNA target sites:

MORC3	GCTGATACTGAGATACCATA**TGG**
scramble	GCTGCTCCCTAACAGGACGC

Extended Data
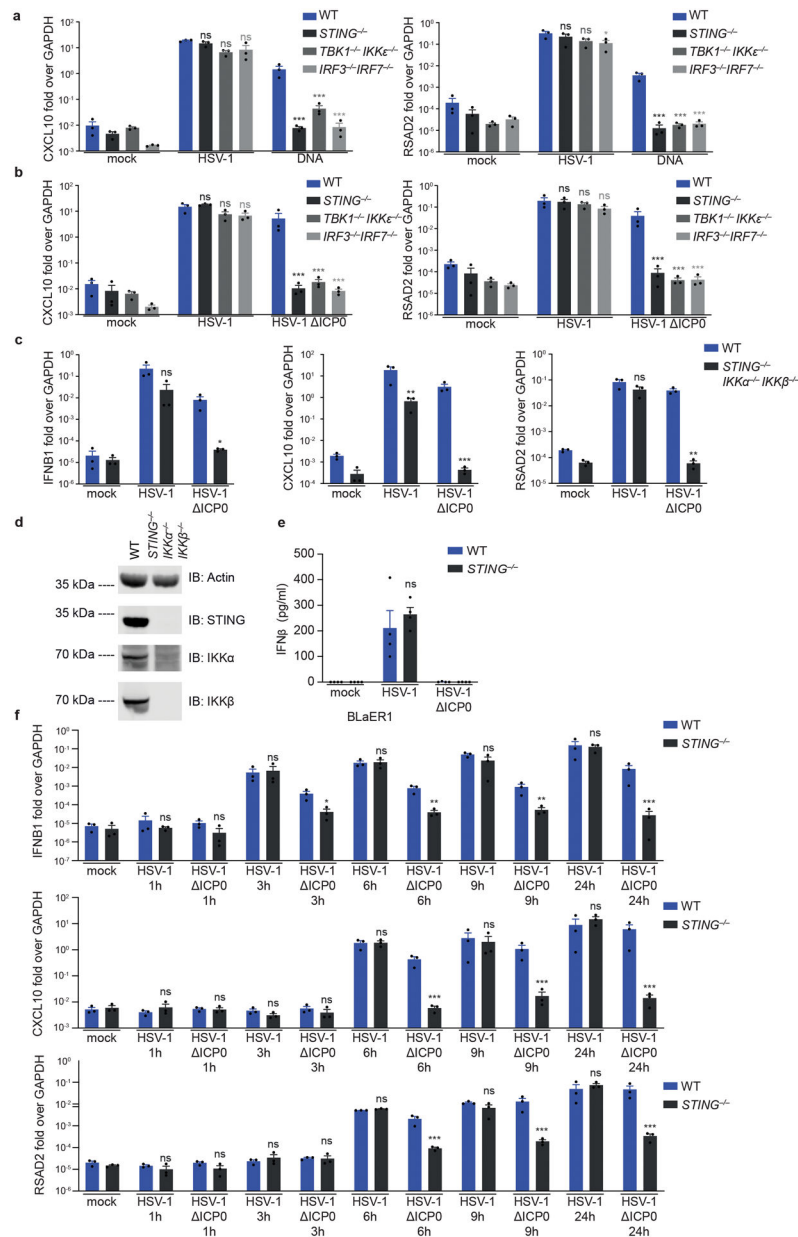
Extended Data Figure 1: Redundancy between DNA- and ICP0-triggered sensing of HSV-1 in BLaER1 monocytes

(a-c) BLaER1 monocytes were infected with HSV-1 at MOI=1 for 24h or transfected with DNA for 3h. Gene-expression analysis is depicted as mean + SEM of three independent experiments.

(d) Immunoblot of BLaER1 monocytes of indicated genotypes.

(e) BLaER1 monocytes were infected with HSV-1 at MOI=1 for 24h and IFNβ secretion was measured by ELISA. Data is depicted as mean + SEM of four independent experiments.

(f) BLaER1 monocytes were infected with HSV-1 at MOI=5. Gene-expression is depicted as mean + SEM of three independent experiments.

* p < 0.05; ** p < 0.01; *** p < 0.001; ns = not significantly different than WT, tested by two-way ANOVA and Dunnett's or Bonferroni's post hoc test. See Source Data for exact p values.
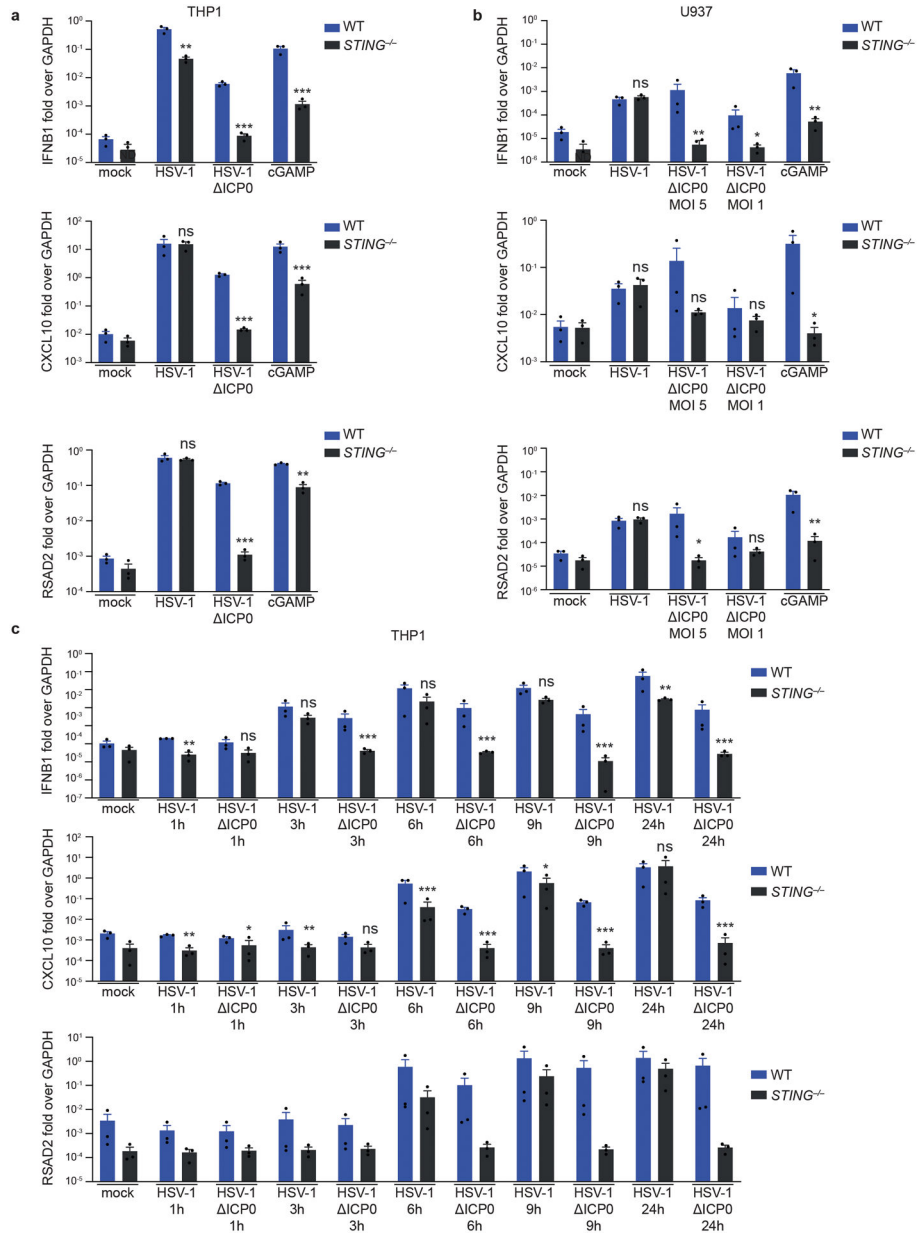
Extended Data Figure 2: Redundancy between DNA- and ICP0-triggered sensing of HSV-1 in THP1 and U937 cells

PMA-differentiated THP1 (a, c) or U937 (b) human myeloid-like cells were infected with HSV-1 at MOI=1 or indicated MOI for 24h (a, b) or indicated timepoints (c) or transfected with 2′-3′-cGAMP for 4h. Gene-expression analysis is depicted as mean + SEM of three independent experiments. ND = not detected. * p < 0.05; ** p < 0.01; *** p < 0.001; ns = not significantly different than WT, tested by two-way ANOVA or Mixed-effects model and Bonferroni's post hoc test. See Source Data for exact p values.
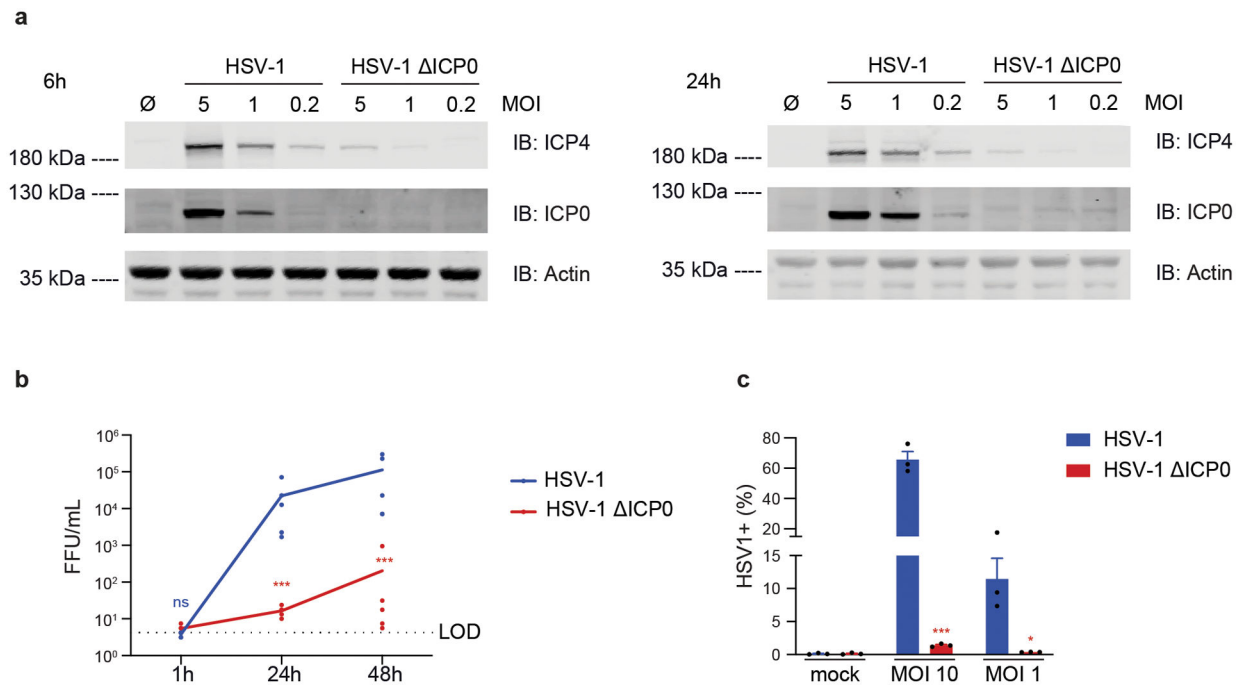
Extended Data Figure 3: HSV-1 ΔICP0 is attenuated in BLaER1 monocytes

(a) BLaER1 monocytes were infected with HSV-1 at indicated MOI and protein expression was analyzed by immunoblot at indicated timepoints. Data is depicted as one representative of two experiments.

(b) BLaER1 monocytes were infected with HSV-1 at MOI=1 and viral progeny was quantified in the supernatant. Mean of five independent experiments is shown.

(c) BLaER1 monocytes were infected with HSV-1 at indicated MOI and analyzed by flow cytometry. Mean + SEM of three independent experiments is depicted. Data is duplicated in Fig. 3b.

* p < 0.05; *** p < 0.001; ns = not significantly different than HSV-1 WT, tested by two-way ANOVA and Bonferroni's post hoc test. See Source Data for exact p values.
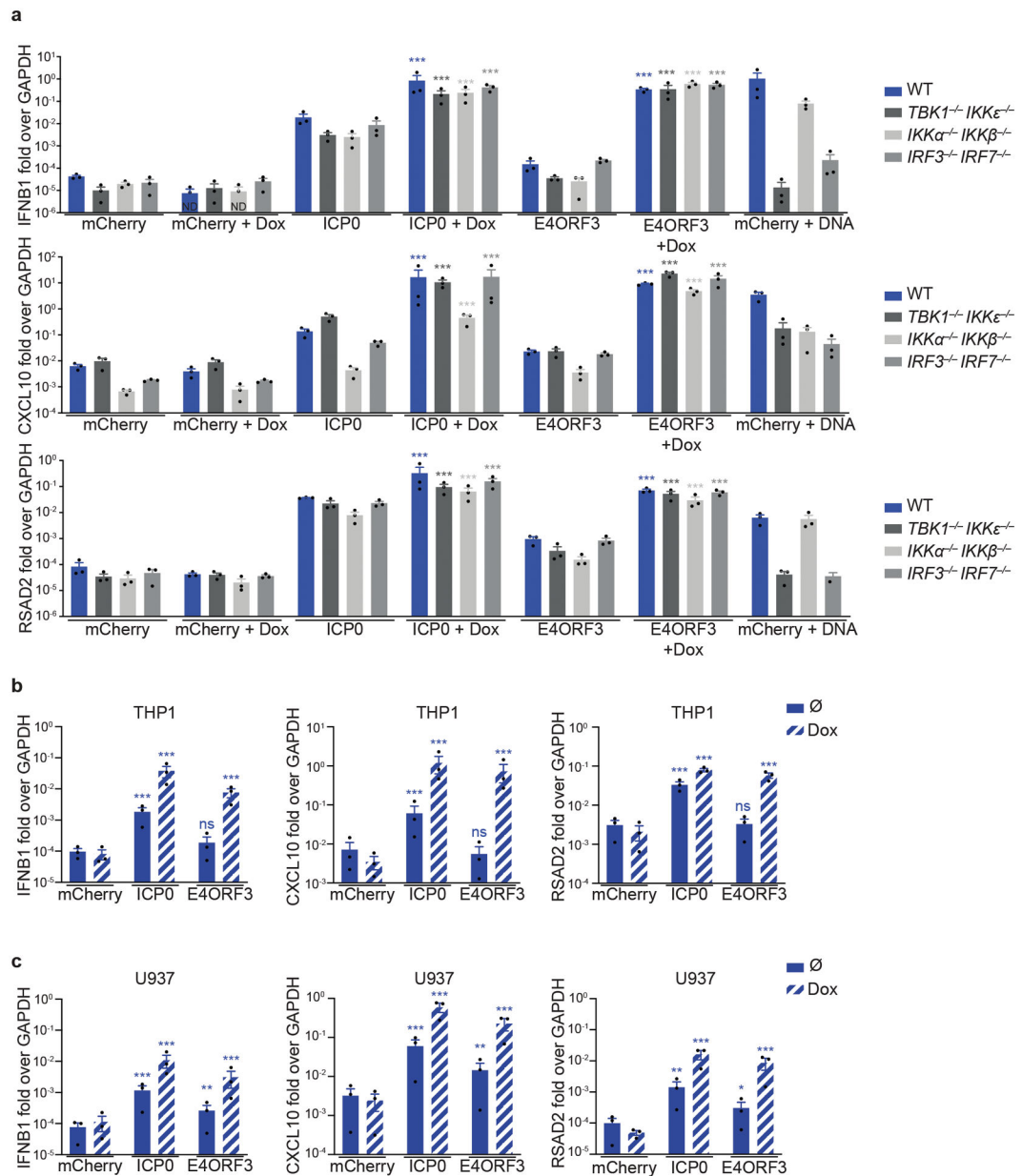
Extended Data Figure 4: Virulence factors induce IFN in monocytes independently of PRR-signaling hubs

BLaER1 monocytes (a), PMA-differentiated THP1 (b) or U937 (c) cells expressing doxycycline-inducible virulence factors were stimulated with doxycycline for 24h, left untreated or stimulated with DNA for 3h. Gene-expression as quantified by q-RT-PCR is depicted as mean + SEM of three independent experiments. *IFNB1* expression levels in a) are partially duplicated from Fig. 1c. * p < 0.05; ** p < 0.01; *** p < 0.001; ns = not significantly different than the corresponding mCherry-expressing condition, tested by two-way ANOVA or Mixed-effects model and Dunnett's post hoc test. ND = not detected. See Source Data for exact p values.
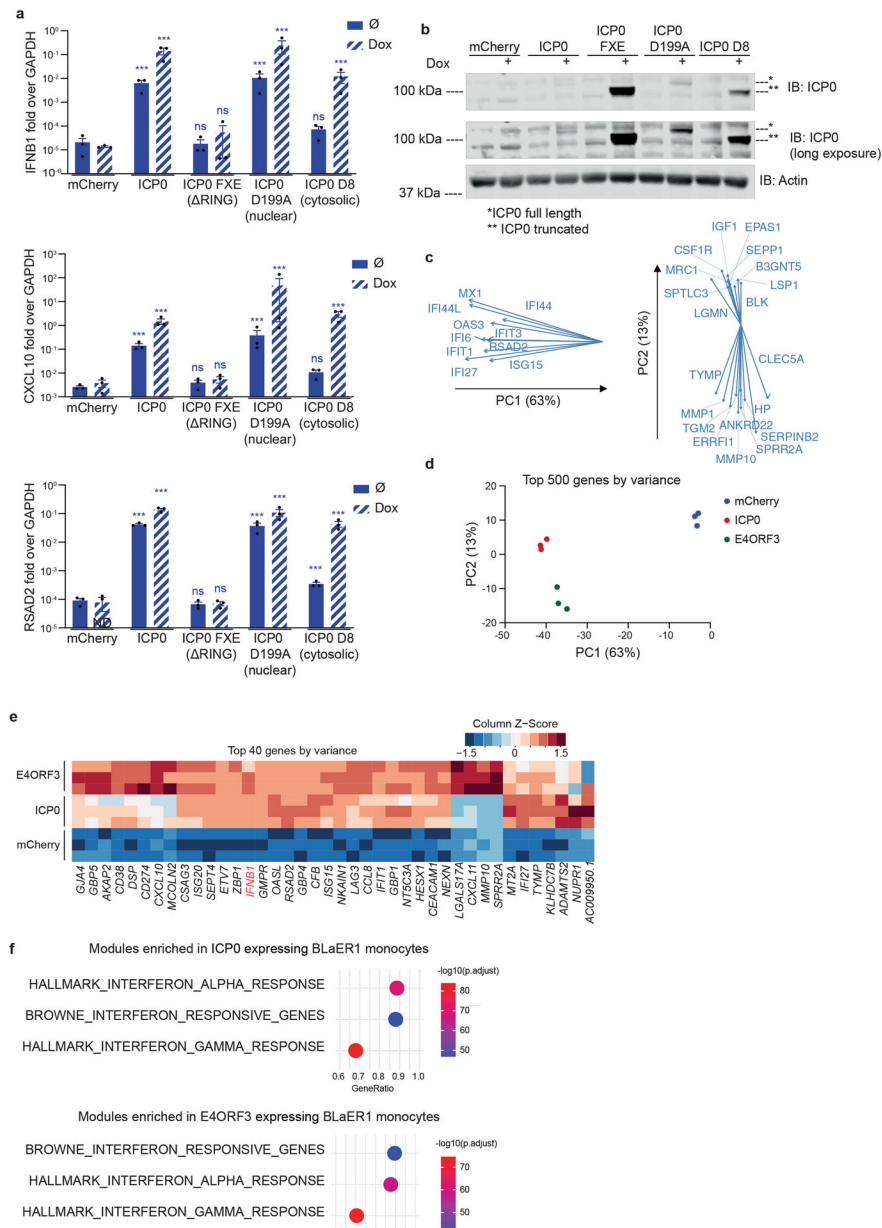
Extended Data Figure 5: Virulence factor activity is required for IFN induction

(a, b) BLaER1 monocytes expressing doxycycline-inducible virulence factors were stimulated with doxycycline for 24h. Gene-expression as quantified by q-RT-PCR is depicted as mean ± SEM of three independent experiments and protein expression by immunoblot is depicted from one representative experiment of two. *** $p < 0.001$; ns = not significantly different than the corresponding mCherry-expressing condition, tested by two-way ANOVA or Mixed-effects model and Dunnett's post hoc test. See Source Data for exact p values.

(c-f) BLaER1 monocytes expressing doxycycline-inducible virulence factors were stimulated with doxycycline for 24h. Transcriptomic changes in BLaER1 monocytes as detected by RNA-seq were analyzed by PCA of variance stabilizing transformed counts.

Top 10 genes that contribute to individual PC directions are depicted (c). Heatmap of log normalized counts of the top 40 most variable genes (column normalized) from three independent RNA-seq experiments is shown (e). Modules from the Molecular Signatures Database that were found to be enriched in differentially expressed genes upon virulence factor expression in BLaER1 monocytes (f). Genes contributing to individual modules can be found in Supplementary Table 1.
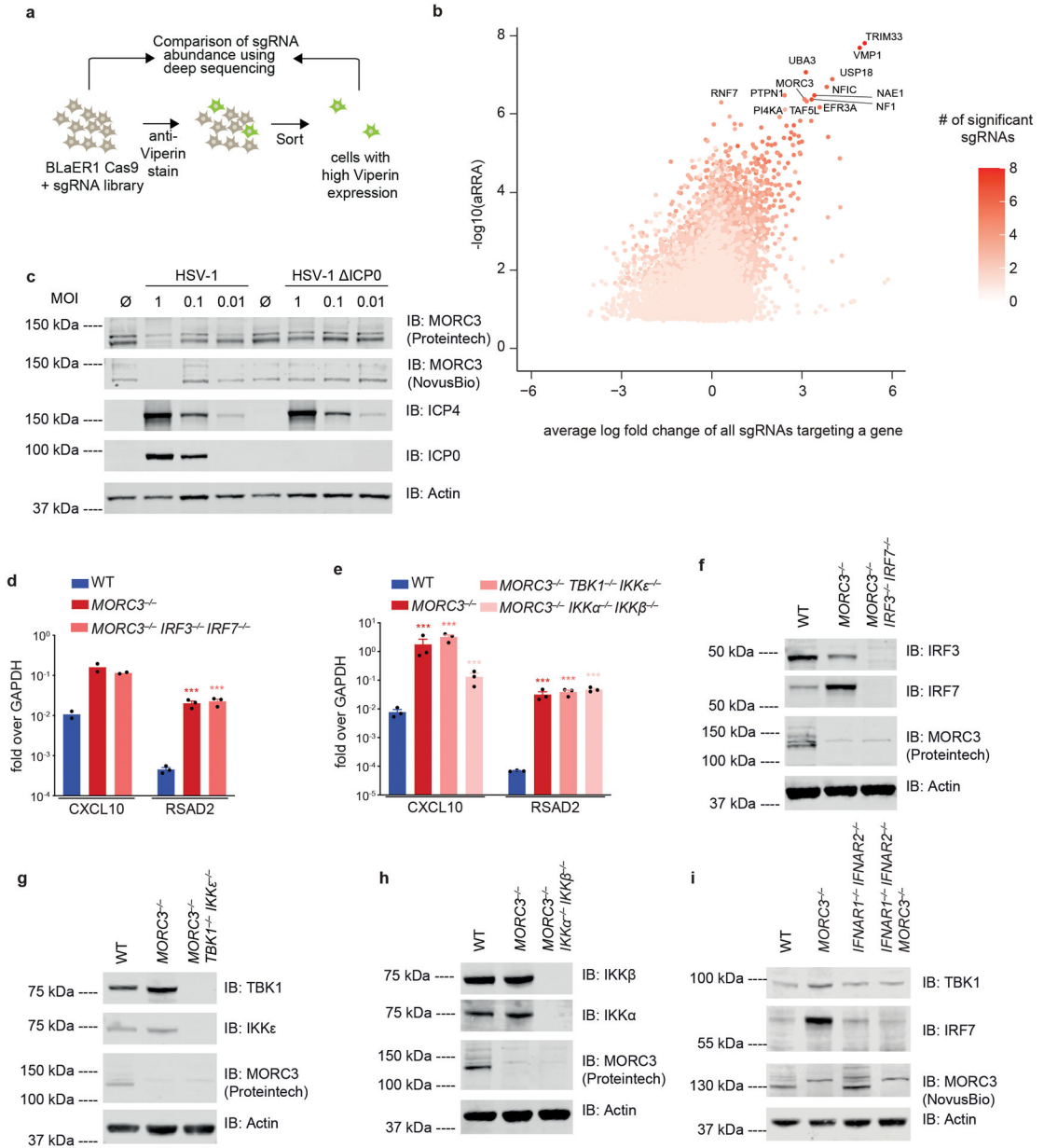
Extended Data Figure 6: Validation of MORC3 as a repressor of IFN
(a) Schematic of a genome wide CRISPR screen to identify negative regulators of IFN.

(b) PinAPL.py analysis of the CRISPR screen to identify negative regulators of IFN. Significantly enriched genes are labeled. Raw data can be found in Supplementary Table 2.

(c) U2OS cells were infected with HSV-1 for 24h. One representative immunoblot of two is shown.

(d, e) Gene expression of BLaER1 monocytes is shown as mean + SEM of 3 independent experiment from one representative clone or two (multiple KOs) or one clone (WT and $MORC3^{-/-}$) except CXCL10 quantification in (d) which is shown as mean of 2 independent experiments. *** $p < 0.001$; significantly different than the corresponding WT condition, tested by two-way ANOVA and Dunnett's post hoc test. See Source Data for exact p values.

(f-i) Immunoblot of BLaER1 monocytes of indicated genotypes.
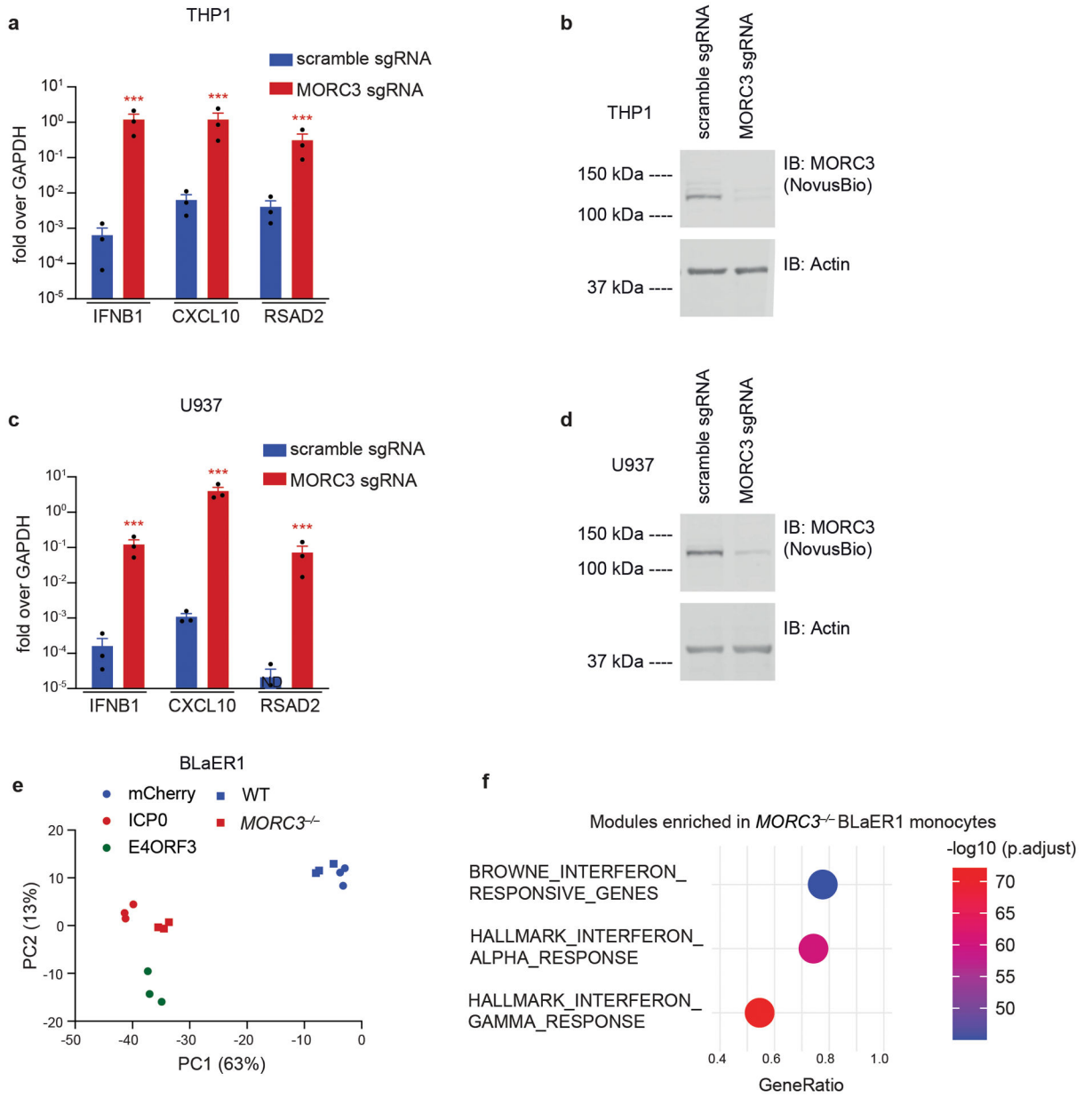
Extended Data Figure 7: Characterization of *MORC3* deficiency in THP1, U937 and BLaER1 cells

(a-d) Gene-expression in PMA-differentiated THP1-Cas9 or PMA-differentiated U937-Cas9 human myeloid-like cells expressing indicated sgRNAs is depicted as mean + SEM of three independent experiments. Protein expression in the same cells was analyzed by immunoblot. ND = not detected. *** $p < 0.001$; ns = not significantly different than the corresponding scramble sgRNA-expressing condition, tested by two-way ANOVA and Bonferroni's post hoc test. See Source Data for exact p values.

(e) Transcriptional changes in BLaER1 monocytes as detected by RNA-seq in three independent experiments are depicted by PCA. These data are partially duplicated from Extended Data Fig. 5d.

(f) Modules from the Molecular Signatures Database that were found to be enriched in differentially expressed genes in *MORC3*$^{-/-}$ BLaER1 monocytes. Background gene set includes all genes that have base mean expression of at least 1 in *MORC3*$^{-/-}$ BLaER1 monocytes. Genes contributing to individual modules can be found in Supplementary Table 1.
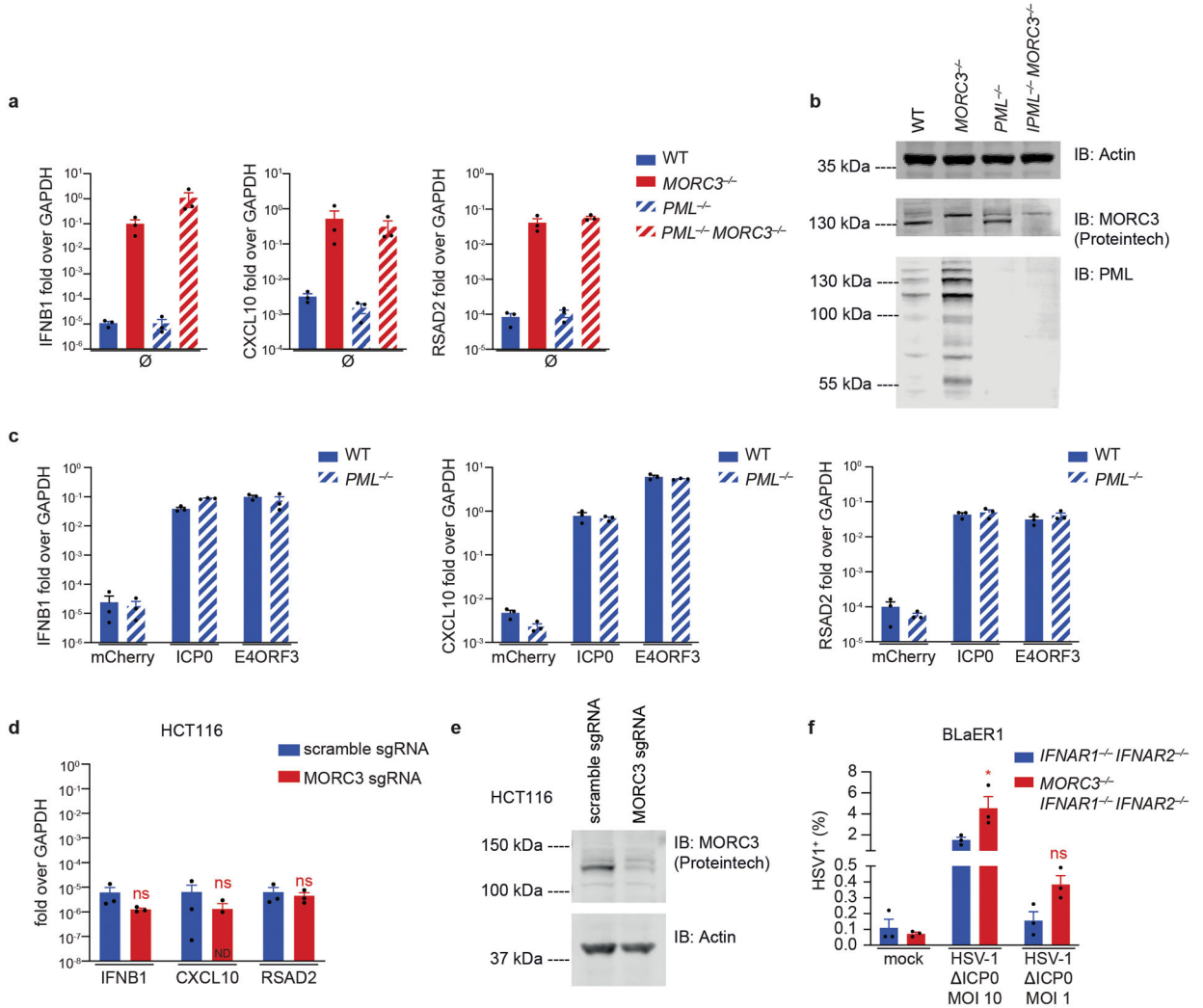
Extended Data Figure 8: PML is not required for IFNB1 regulation by MORC3

(a) Gene expression of BLaER1 monocytes of indicated genotype is depicted as mean + SEM of three independent experiments.

(b) Protein expression of BLaER1 monocytes was analyzed by immunoblot.

(c) BLaER1 monocytes expressing doxycycline-inducible virulence factors were stimulated with doxycycline for 24h. Gene-expression as quantified by q-RT-PCR is depicted as mean + SEM of three independent experiments.

(d, e) Gene-expression in HCT116-Cas9 cells expressing indicated sgRNAs is depicted as mean + SEM of three independent experiments. Protein expression in the same cells was analyzed by immunoblot. ND = not detected. ns = not significantly different than the

corresponding scramble sgRNA-expressing condition, tested by Mixed-effects model and Bonferroni's post hoc test. See Source Data for exact p values.

(f) BLaER1 monocytes of indicated genotype were infected with ICP0 HSV-1 at indicated MOI for 6h and analyzed by flow cytometry. Mean + SEM of three independent experiment is depicted. * p < 0.05 ; ns = not significantly different than the *IFNAR1*$^{-/-}$*IFNAR2*$^{-/-}$ condition, tested by two-way ANOVA and Bonferroni's post hoc test. See Source Data for exact p values.
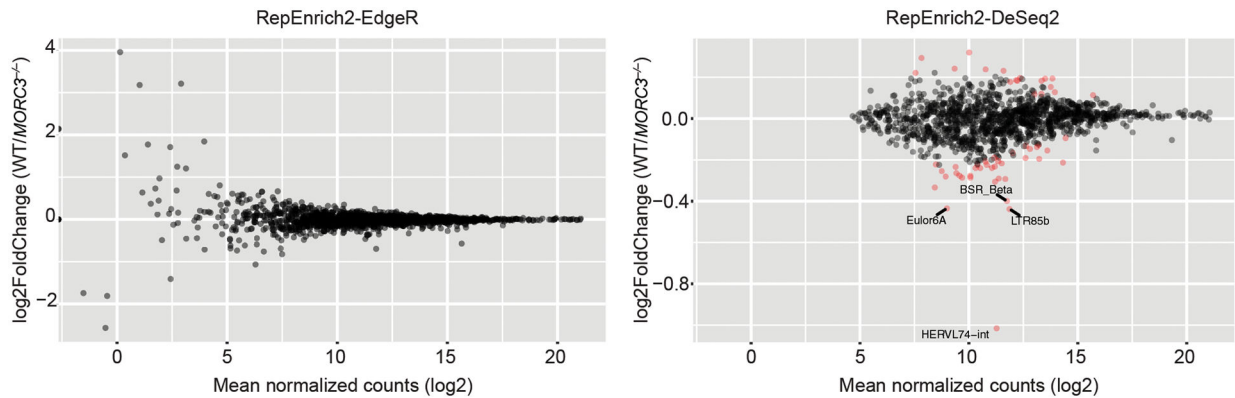
Extended Data Figure 9: Quantification of expression of ERV families

ERV family expression was quantified with RepEnrich2 in *IFNAR1*$^{-/-}$*IFNAR2*$^{-/-}$ mCherry vs *MORC3*$^{-/-}$*IFNAR1*$^{-/-}$*IFNAR2*$^{-/-}$ monocytes. ERVs with an FDR <0.05 are highlighted in red. The recommended RepEnrich2-EdgeR pipeline did not detect any regulation of ERVs upon *MORC3* deficiency. RepEnrich2-DeSeq2 analysis suggested minimal up- and down-regulation of ERV families. The only strongly de-repressed ERV family upon *MORC3* deficiency includes members within the MORC3-repressed region on chromosome 9, consistent with a positional rather than an ERV-specific de-repression.
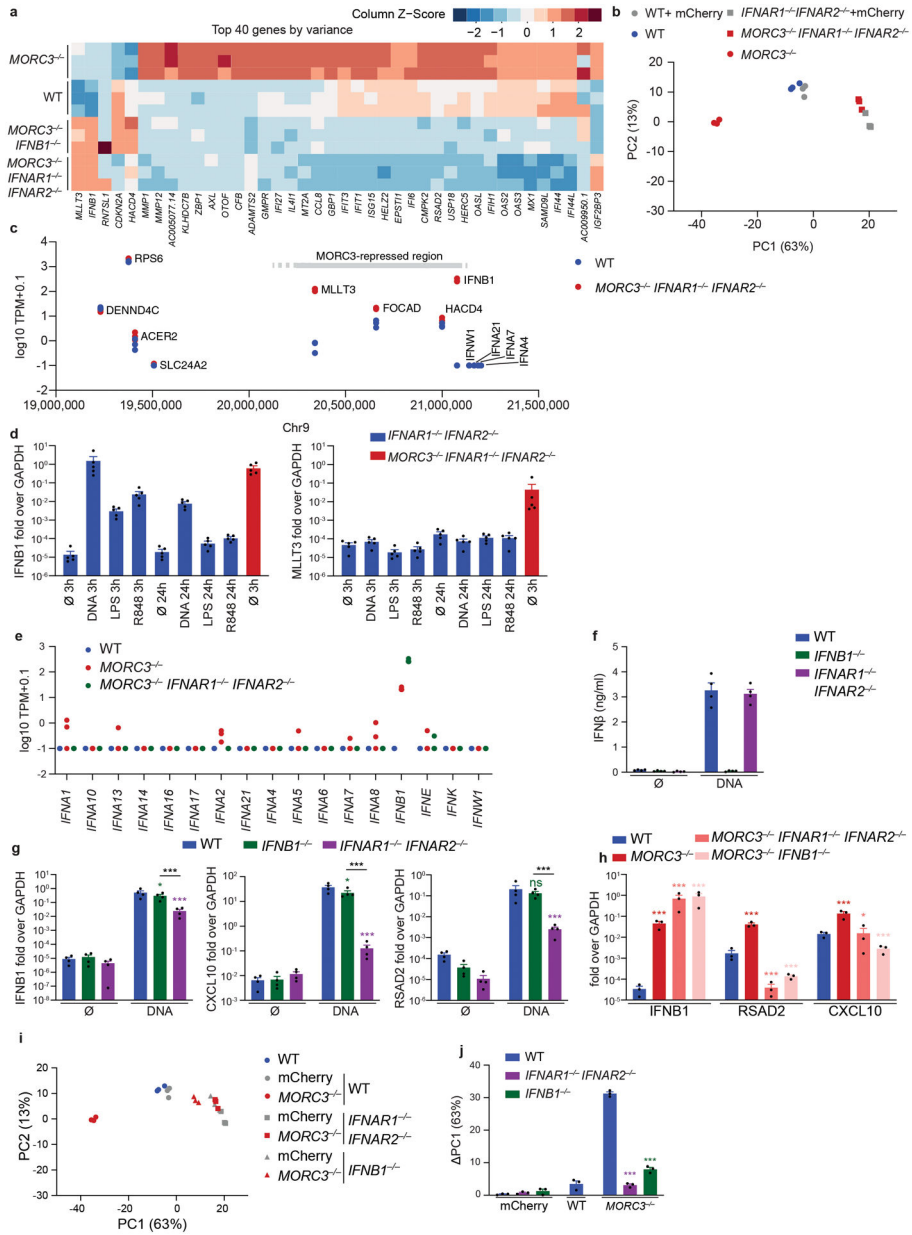
**Extended Data Figure 10: *MORC3* deficiency leads to de-repression of a gene cluster at chromosome 9**

(a) Column-normalized heatmap analysis of transcriptomic changes in BLaER1 monocytes as detected by RNA-seq in three independent experiments.

(b) Transcriptional changes in BLaER1 monocytes as detected by RNA-seq in three independent experiments are depicted by PCA. These data are partially duplicated from Extended Data Fig. 7e.

(c) Log transcripts per million (TPM) of genes in BLaER1 monocytes of genes clustered near *IFNB1* on chromosome 9 as detected by RNA-seq from three independent experiments. All protein coding genes within this region are depicted.

(d) BLaER1 monocytes were stimulated with indicated PAMPs for 3h or 24h. Gene-expression analysis is depicted as mean + SEM of five independent experiments.

(e) Log transcripts per million (TPM) of IFN genes in BLaER1 monocytes were detected by RNAseq in three independent experiments.

(f, g) BLaER1 monocytes were stimulated with DNA for 12h or left untreated. Cytokine secretion or gene expression from one representative clone of two per genotype except WT is shown as mean + SEM of four (f) or three (g) independent experiments. * p < 0.05 ; *** p < 0.001; ns = not significantly different than WT (unless otherwise indicated), tested by two-way ANOVA and Bonferroni's post hoc test. See Source Data for exact p values.

(h) Gene expression from BLaER1 monocytes of indicated genotypes is depicted as mean + SEM of three independent experiments. *** p < 0.001; ns = not significantly different than WT, tested by two-way ANOVA and Dunnett's post hoc test. See Source Data for exact p values.

(i, j) Transcriptomic changes in BLaER1 monocytes as detected by RNA-seq in three independent experiments are depicted by PCA. The data in (i) is partially duplicated from (b). The distance on PC1-axis between samples and the mean of mCherry-expressing cells was calculated and is depicted as mean + SEM from three independent experiments. *** p < 0.001 significantly different than WT, tested by two-way ANOVA and Dunnett's post hoc test. See Source Data for exact p values.
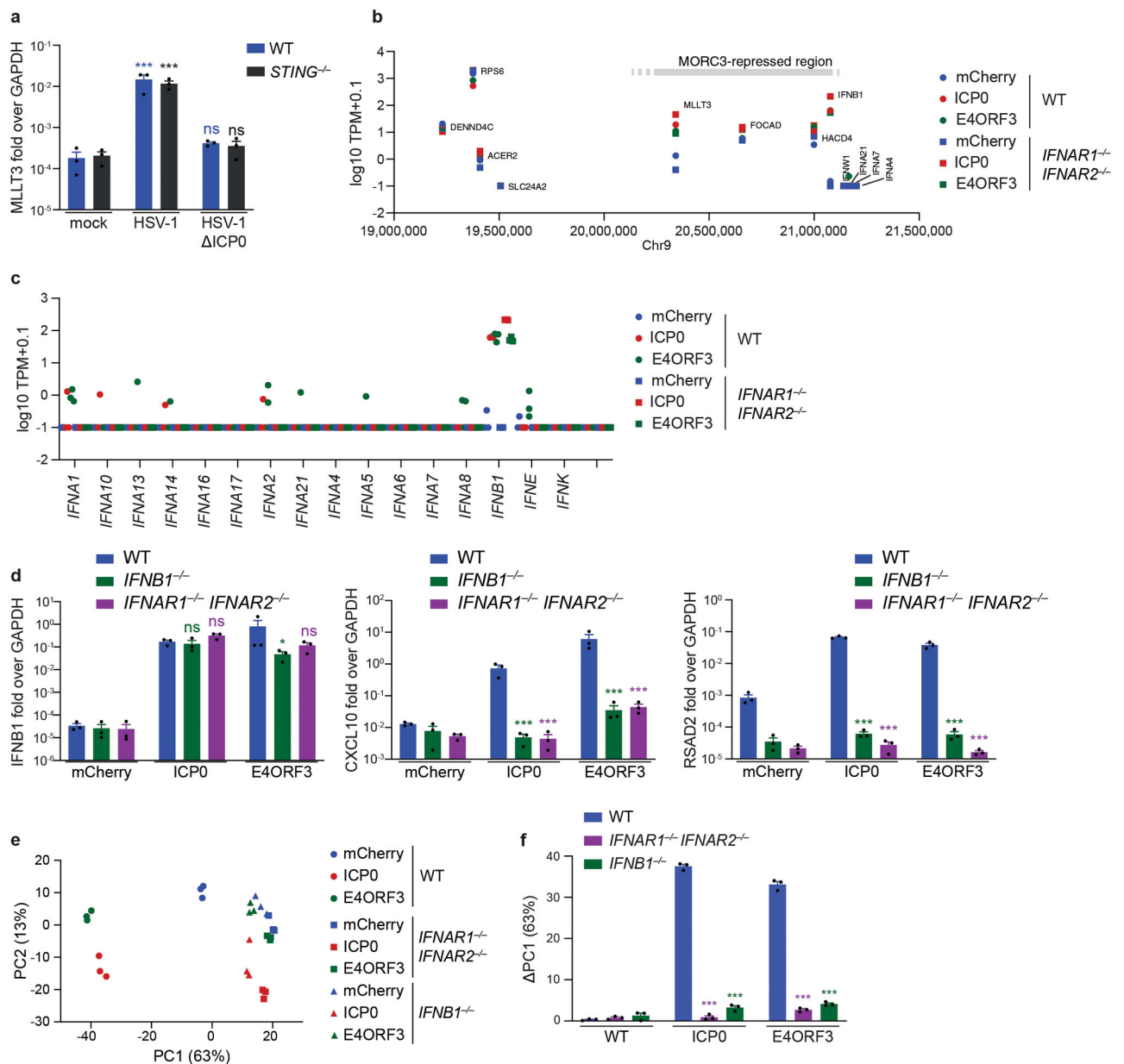
**Extended Data Figure 11: Positional de-repression of *IFNB1* explains IFN induction by virulence factors**

(a) BLaER1 monocytes were infected with HSV-1 at MOI=1 for 24h. *MLLT3* expression is depicted as mean + SEM of n=3 independent experiments. *** p < 0.001; ns = not significantly different than mock infection, tested by two-way ANOVA and Dunnett's post hoc test. See Source Data for exact p values.

(b) Mean log transcripts per million (TPM) of a gene cluster at chromosome 9 in BLaER1 monocytes. Mean TPM is calculated for each condition across three independent experiments. All protein coding genes within this region are depicted.

(c) Log transcripts per million (TPM) of IFN genes in BLaER1 monocytes upon virulence factor expression were detected by RNAseq in three independent experiments.

(d) BLaER1 monocytes expressing doxycycline-inducible virulence factors were stimulated with doxycycline for 24h. Gene expression is shown as mean + SEM of n=3 independent experiments. ** $p < 0.01$; *** $p < 0.001$; ns = not significantly different than WT, tested by two-way ANOVA and Dunnett's post hoc test. See Source Data for exact p values. Note that $IFNB1^{-/-}$ cells harbor small indels within $IFNB1$ that allow detection of mRNA by q-RT-PCR.

(e,f) BLaER1 monocytes expressing doxycycline-inducible virulence factors were stimulated with doxycycline for 24h. Transcriptomic changes as detected by RNA-seq in three independent experiments were analyzed PCA. Data is partially duplicated from Extended Data Fig. 10i. The distance on PC1-axis between samples and the mean of mCherry-expressing cells was calculated and is depicted as mean + SEM from three independent experiments. *** $p < 0.001$ significantly different than WT, tested by two-way ANOVA and Dunnett's post hoc test. See Source Data for exact p values.
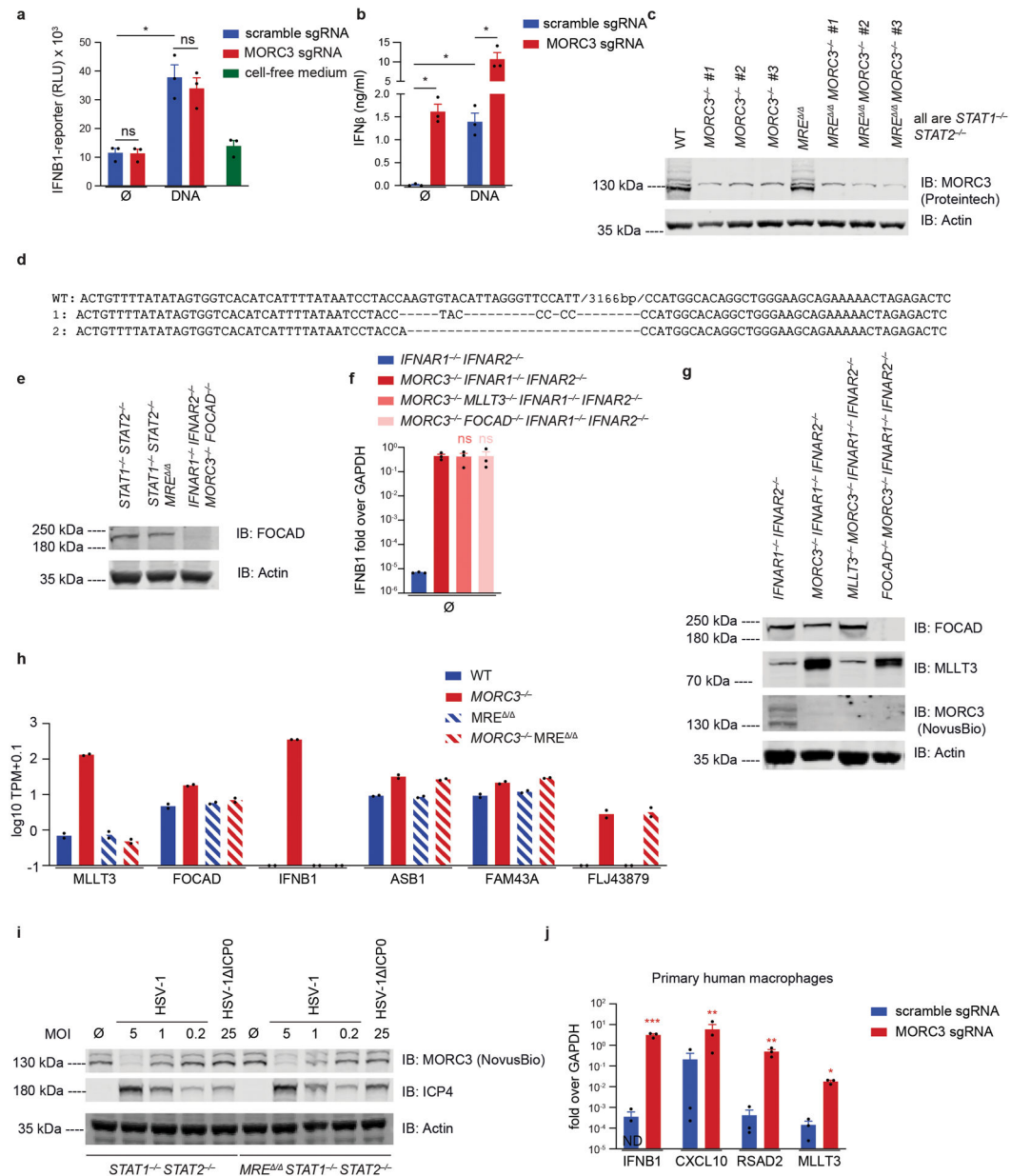
Extended Data Figure 12: Validation of the MORC3-regulated DNA element

(a, b) $STAT1^{-/-}STAT2^{-/-}$BLaER1-Cas9 expressing a randomly integrated *IFNB1*-promoter-Luciferase reporter were transduced with the indicated sgRNAs and stimulated with cytosolic DNA for 24h. Luciferase signal and IFNβ secretion is depicted as mean + SEM of n=3 independent experiments. * p < 0.05; ns = not significantly different, tested by paired, two-sided t-test. See Source Data for exact p values.

(c) Protein expression of indicated BLaER1 monocytes was analyzed by immunoblot. This experiment was performed once.

(d) Consensus sequences of amplicon sequencing at the MRE locus from $STAT1^{-/-}STAT2^{-/-}$ $MRE^{/}$ BLaER1 Cas9 cells were aligned to the WT reference. 3166bp were omitted from the reference sequence.

(e) Protein expression of indicated BLaER1 monocytes was analyzed by immunoblot. One representative experiment of two is depicted.

(f) Gene expression of indicated BLaER1 monocytes is depicted as mean + SEM of three independent experiments from one representative clone of two ($MORC3^{-/-}$ $MLLT3^{-/-}$ $IFNAR1^{-/-}$ $IFNAR2^{-/-}$ and $MORC3^{-/-}$ $FOCAD^{-/-}$ $IFNAR1^{-/-}$ $IFNAR2^{-/-}$) or one ($IFNAR1^{-/-}IFNAR2^{-/-}$ and $MORC3^{-/-}IFNAR1^{-/-}IFNAR2^{-/-}$) per genotype. ns = not significantly different than the $IFNAR1^{-/-}IFNAR2^{-/-}$ condition, tested by two-way ANOVA and Dunnett's post hoc test. See Source Data for exact p values.

(g) Protein expression of indicated BLaER1 monocytes was analyzed by immunoblot. This experiment was performed once.

(h) Log transcripts per million (TPM) of high-confidence MORC3 targets (genes de-repressed in $MORC3^{-/-}$ $IFNAR1^{-/-}IFNAR2^{-/-}$, $MORC3^{-/-}$ $IFNB1^{-/-}$ and $MORC3^{-/-}$ $STAT1^{-/-}STAT2^{-/-}$ Cas9) in WT = $MORC3^{-/-}$ $STAT1^{-/-}STAT2^{-/-}$ Cas9 or indicated genotypes are depicted as mean of two independent RNA-seq experiments.

(i) $STAT1^{-/-}STAT2^{-/-}$ Cas9 ("WT") or $STAT1^{-/-}STAT2^{-/-}$ $MRE^{\ /}$ BLaER1 Cas9 were infected with HSV-1 at indicated MOI for 4–5h. One representative immunoblot of two is depicted.

(j) Peripheral blood human monocytes were nucleofected with indicated sgRNA:Cas9 complexes and differentiated with M-CSF for 5 days. Gene expression from three independent donors is depicted as mean + SEM. * $p < 0.05$; ** $p < 0.01$; *** $p < 0.001$; significantly different than the scramble sgRNA condition, tested by two-way ANOVA and Bonferroni's post hoc test. ND = not detected. Source Data for exact p values.

Supplementary Material

Refer to Web version on PubMed Central for supplementary material.

Acknowledgments

Data availability

RNA-seq and ATAC-seq data that support the findings of the study have been deposited in the Gene Expression Omnibus under accession no. GSE183011. CRISPR/Cas9 screen data has been deposited in the Sequence Read Archive under accession no. PRJNA759267. Source data for all figures has been provided in the source data file.

REFERENCES

1. Lopes Fischer N, Naseer N, Shin S & Brodsky IE Effector-triggered immunity and pathogen sensing in metazoans. Nat Microbiol 5, 14–26, doi:10.1038/s41564-019-0623-2 (2020). [PubMed: 31857733]

2. Jones JD & Dangl JL The plant immune system. Nature 444, 323–329, doi:10.1038/nature05286 (2006). [PubMed: 17108957]

3. Van der Biezen EA & Jones JD Plant disease-resistance proteins and the gene-for-gene concept. Trends Biochem Sci 23, 454–456, doi:10.1016/s0968-0004(98)01311-5 (1998). [PubMed: 9868361]

4. Sloan E et al. Analysis of the SUMO2 Proteome during HSV-1 Infection. PLoS Pathog 11, e1005059, doi:10.1371/journal.ppat.1005059 (2015). [PubMed: 26200910]

5. Sloan E, Orr A & Everett RD MORC3, a Component of PML Nuclear Bodies, Has a Role in Restricting Herpes Simplex Virus 1 and Human Cytomegalovirus. J Virol 90, 8621–8633, doi:10.1128/JVI.00621-16 (2016). [PubMed: 27440897]

6. Janeway CA Jr. Approaching the asymptote? Evolution and revolution in immunology. Cold Spring Harb Symp Quant Biol 54 Pt 1, 1–13, doi:10.1101/sqb.1989.054.01.003 (1989).

7. Hopfner KP & Hornung V Molecular mechanisms and cellular functions of cGAS-STING signalling. Nat Rev Mol Cell Biol 21, 501–521, doi:10.1038/s41580-020-0244-x (2020). [PubMed: 32424334]

8. Ishikawa H, Ma Z & Barber GN STING regulates intracellular DNA-mediated, type I interferon-dependent innate immunity. Nature 461, 788–792, doi:10.1038/nature08476 (2009). [PubMed: 19776740]

9. Scherer M & Stamminger T Emerging Role of PML Nuclear Bodies in Innate Immune Signaling. J Virol 90, 5850–5854, doi:10.1128/JVI.01979-15 (2016). [PubMed: 27053550]

10. Everett RD, Boutell C & Hale BG Interplay between viruses and host sumoylation pathways. Nat Rev Microbiol 11, 400–411, doi:10.1038/nrmicro3015 (2013). [PubMed: 23624814]

11. Sacks WR & Schaffer PA Deletion mutants in the gene encoding the herpes simplex virus type 1 immediate-early protein ICP0 exhibit impaired growth in cell culture. J Virol 61, 829–839, doi:10.1128/JVI.61.3.829-839.1987 (1987). [PubMed: 3027408]

12. Rapino F et al. C/EBPalpha induces highly efficient macrophage transdifferentiation of B lymphoma and leukemia cell lines and impairs their tumorigenicity. Cell Rep 3, 1153–1163, doi:10.1016/j.celrep.2013.03.003 (2013). [PubMed: 23545498]

13. Ullman AJ & Hearing P Cellular proteins PML and Daxx mediate an innate antiviral defense antagonized by the adenovirus E4 ORF3 protein. J Virol 82, 7325–7335, doi:10.1128/JVI.00723-08 (2008). [PubMed: 18480450]

14. Everett RD Construction and characterization of herpes simplex virus type 1 mutants with defined lesions in immediate early gene 1. J Gen Virol 70 (Pt 5), 1185–1202, doi:10.1099/0022-1317-70-5-1185 (1989). [PubMed: 2543774]

15. Lopez P, Van Sant C & Roizman B Requirements for the nuclear-cytoplasmic translocation of infected-cell protein 0 of herpes simplex virus 1. J Virol 75, 3832–3840, doi:10.1128/JVI.75.8.3832-3840.2001 (2001). [PubMed: 11264372]

16. Crowl JT & Stetson DB SUMO2 and SUMO3 redundantly prevent a noncanonical type I interferon response. Proc Natl Acad Sci U S A 115, 6798–6803, doi:10.1073/pnas.1802114115 (2018). [PubMed: 29891701]

17. Decque A et al. Sumoylation coordinates the repression of inflammatory and anti-viral gene-expression programs during innate sensing. Nat Immunol 17, 140–149, doi:10.1038/ni.3342 (2016). [PubMed: 26657003]

18. Ferri F et al. TRIM33 switches off Ifnb1 gene transcription during the late phase of macrophage activation. Nat Commun 6, 8900, doi:10.1038/ncomms9900 (2015). [PubMed: 26592194]

19. Malakhova OA et al. UBP43 is a novel regulator of interferon signaling independent of its ISG15 isopeptidase activity. EMBO J 25, 2358–2367, doi:10.1038/sj.emboj.7601149 (2006). [PubMed: 16710296]

20. Jadhav G, Teguh D, Kenny J, Tickner J & Xu J Morc3 mutant mice exhibit reduced cortical area and thickness, accompanied by altered haematopoietic stem cells niche and bone cell differentiation. Sci Rep 6, 25964, doi:10.1038/srep25964 (2016). [PubMed: 27188231]

21. Li DQ, Nair SS & Kumar R The MORC family: new epigenetic regulators of transcription and DNA damage response. Epigenetics 8, 685–693, doi:10.4161/epi.24976 (2013). [PubMed: 23804034]

22. Rosendorff A et al. NXP-2 association with SUMO-2 depends on lysines required for transcriptional repression. Proc Natl Acad Sci U S A 103, 5308–5313, doi:10.1073/pnas.0601066103 (2006). [PubMed: 16567619]

23. Mimura Y, Takahashi K, Kawata K, Akazawa T & Inoue N Two-step colocalization of MORC3 with PML nuclear bodies. J Cell Sci 123, 2014–2024, doi:10.1242/jcs.063586 (2010). [PubMed: 20501696]

24. Ver LS, Marcos-Villar L, Landeras-Bueno S, Nieto A & Ortin J The Cellular Factor NXP2/MORC3 Is a Positive Regulator of Influenza Virus Multiplication. J Virol 89, 10023–10030, doi:10.1128/JVI.01530-15 (2015). [PubMed: 26202233]

25. Zhang Y et al. MORC3 Is a Target of the Influenza A Viral Protein NS1. Structure 27, 1029–1033 e1023, doi:10.1016/j.str.2019.03.015 (2019). [PubMed: 31006586]

26. Groh S et al. Morc3 silences endogenous retroviruses by enabling Daxx-mediated H3.3 incorporation. bioRxiv, 2020.2011.2012.380204, doi:10.1101/2020.11.12.380204 (2020).

27. Yu P et al. Nucleic acid-sensing Toll-like receptors are essential for the control of endogenous retrovirus viremia and ERV-induced tumors. Immunity 37, 867–879, doi:10.1016/j.immuni.2012.07.018 (2012). [PubMed: 23142781]

28. Lopez-Flores I & Garrido-Ramos MA The repetitive DNA content of eukaryotic genomes. Genome Dyn 7, 1–28, doi:10.1159/000337118 (2012). [PubMed: 22759811]

29. Gaidt MM et al. Human Monocytes Engage an Alternative Inflammasome Pathway. Immunity 44, 833–846, doi:10.1016/j.immuni.2016.01.012 (2016). [PubMed: 27037191]

30. Gaidt MM et al. The DNA Inflammasome in Human Myeloid Cells Is Initiated by a STING-Cell Death Program Upstream of NLRP3. Cell 171, 1110–1124 e1118, doi:10.1016/j.cell.2017.09.039 (2017). [PubMed: 29033128]

31. Blaho JA, Morton ER & Yedowitz JC Herpes simplex virus: propagation, quantification, and storage. Curr Protoc Microbiol Chapter 14, Unit 14E 11, doi:10.1002/9780471729259.mc14e01s00 (2005).

32. Schmidt T, Schmid-Burgk JL, Ebert TS, Gaidt MM & Hornung V Designer Nuclease-Mediated Generation of Knockout THP1 Cells. Methods Mol Biol 1338, 261–272, doi:10.1007/978-1-4939-2932-0_19 (2016). [PubMed: 26443227]

33. Schmid-Burgk JL et al. OutKnocker: a web tool for rapid and simple genotyping of designer nuclease edited cell lines. Genome Res 24, 1719–1723, doi:10.1101/gr.176701.114 (2014). [PubMed: 25186908]

34. Labun K et al. CHOPCHOP v3: expanding the CRISPR web toolbox beyond genome editing. Nucleic Acids Res 47, W171–W174, doi:10.1093/nar/gkz365 (2019). [PubMed: 31106371]

35. Schmidt T, Schmid-Burgk JL & Hornung V Synthesis of an arrayed sgRNA library targeting the human genome. Sci Rep 5, 14987, doi:10.1038/srep14987 (2015). [PubMed: 26446710]

36. Sanjana NE, Shalem O & Zhang F Improved vectors and genome-wide libraries for CRISPR screening. Nat Methods 11, 783–784, doi:10.1038/nmeth.3047 (2014). [PubMed: 25075903]

37. Bartok E et al. iGLuc: a luciferase-based inflammasome and protease activity reporter. Nat Methods 10, 147–154, doi:10.1038/nmeth.2327 (2013). [PubMed: 23291722]

38. Spahn PN et al. PinAPL-Py: A comprehensive web-application for the analysis of CRISPR/Cas9 screens. Sci Rep 7, 15854, doi:10.1038/s41598-017-16193-9 (2017). [PubMed: 29158538]

39. Andrews S FastQC: A Quality Control Tool for High Throughput Sequence Data. (2010).

40. Langmead B & Salzberg SL Fast gapped-read alignment with Bowtie 2. Nat Methods 9, 357–359, doi:10.1038/nmeth.1923 (2012). [PubMed: 22388286]

41. Li B & Dewey CN RSEM: accurate transcript quantification from RNA-Seq data with or without a reference genome. BMC Bioinformatics 12, 323, doi:10.1186/1471-2105-12-323 (2011). [PubMed: 21816040]

42. Love MI, Huber W & Anders S Moderated estimation of fold change and dispersion for RNA-seq data with DESeq2. Genome Biol 15, 550, doi:10.1186/s13059-014-0550-8 (2014). [PubMed: 25516281]

43. Yu G, Wang LG, Han Y & He QY clusterProfiler: an R package for comparing biological themes among gene clusters. OMICS 16, 284–287, doi:10.1089/omi.2011.0118 (2012). [PubMed: 22455463]

44. Liberzon A et al. Molecular signatures database (MSigDB) 3.0. Bioinformatics 27, 1739–1740, doi:10.1093/bioinformatics/btr260 (2011). [PubMed: 21546393]

45. Buenrostro JD, Wu B, Chang HY & Greenleaf WJ ATAC-seq: A Method for Assaying Chromatin Accessibility Genome-Wide. Curr Protoc Mol Biol 109, 21 29 21–21 29 29, doi:10.1002/0471142727.mb2129s109 (2015).

46. Martin M Cutadapt removes adapter sequences from high-throughput sequencing reads. 2011 17, 3, doi:10.14806/ej.17.1.200 (2011).

47. Li H et al. The Sequence Alignment/Map format and SAMtools. Bioinformatics 25, 2078–2079, doi:10.1093/bioinformatics/btp352 (2009). [PubMed: 19505943]

48. BroadInstitute. Picard Toolkit, <http://broadinstitute.github.io/picard/> (2018).

49. Amemiya HM, Kundaje A & Boyle AP The ENCODE Blacklist: Identification of Problematic Regions of the Genome. Sci Rep 9, 9354, doi:10.1038/s41598-019-45839-z (2019). [PubMed: 31249361]

50. Buenrostro JD, Giresi PG, Zaba LC, Chang HY & Greenleaf WJ Transposition of native chromatin for fast and sensitive epigenomic profiling of open chromatin, DNA-binding proteins and nucleosome position. Nat Methods 10, 1213–1218, doi:10.1038/nmeth.2688 (2013). [PubMed: 24097267]

51. Zhang Y et al. Model-based analysis of ChIP-Seq (MACS). Genome Biol 9, R137, doi:10.1186/gb-2008-9-9-r137 (2008). [PubMed: 18798982]

52. Cavalcante RG & Sartor MA annotatr: genomic regions in context. Bioinformatics 33, 2381–2383, doi:10.1093/bioinformatics/btx183 (2017). [PubMed: 28369316]

53. Dobin A et al. STAR: ultrafast universal RNA-seq aligner. Bioinformatics 29, 15–21, doi:10.1093/bioinformatics/bts635 (2013). [PubMed: 23104886]

54. Criscione SW, Zhang Y, Thompson W, Sedivy JM & Neretti N Transcriptional landscape of repetitive elements in normal and cancer human cells. BMC Genomics 15, 583, doi:10.1186/1471-2164-15-583 (2014). [PubMed: 25012247]

55. nerettilab. RepEnrich2. https://github.com/nerettilab/RepEnrich2 (2019).

56. Robinson MD, McCarthy DJ & Smyth GK edgeR: a Bioconductor package for differential expression analysis of digital gene expression data. Bioinformatics 26, 139–140, doi:10.1093/bioinformatics/btp616 (2010). [PubMed: 19910308]

57. Freund EC et al. Efficient gene knockout in primary human and murine myeloid cells by non-viral delivery of CRISPR-Cas9. J Exp Med 217, doi:10.1084/jem.20191692 (2020).
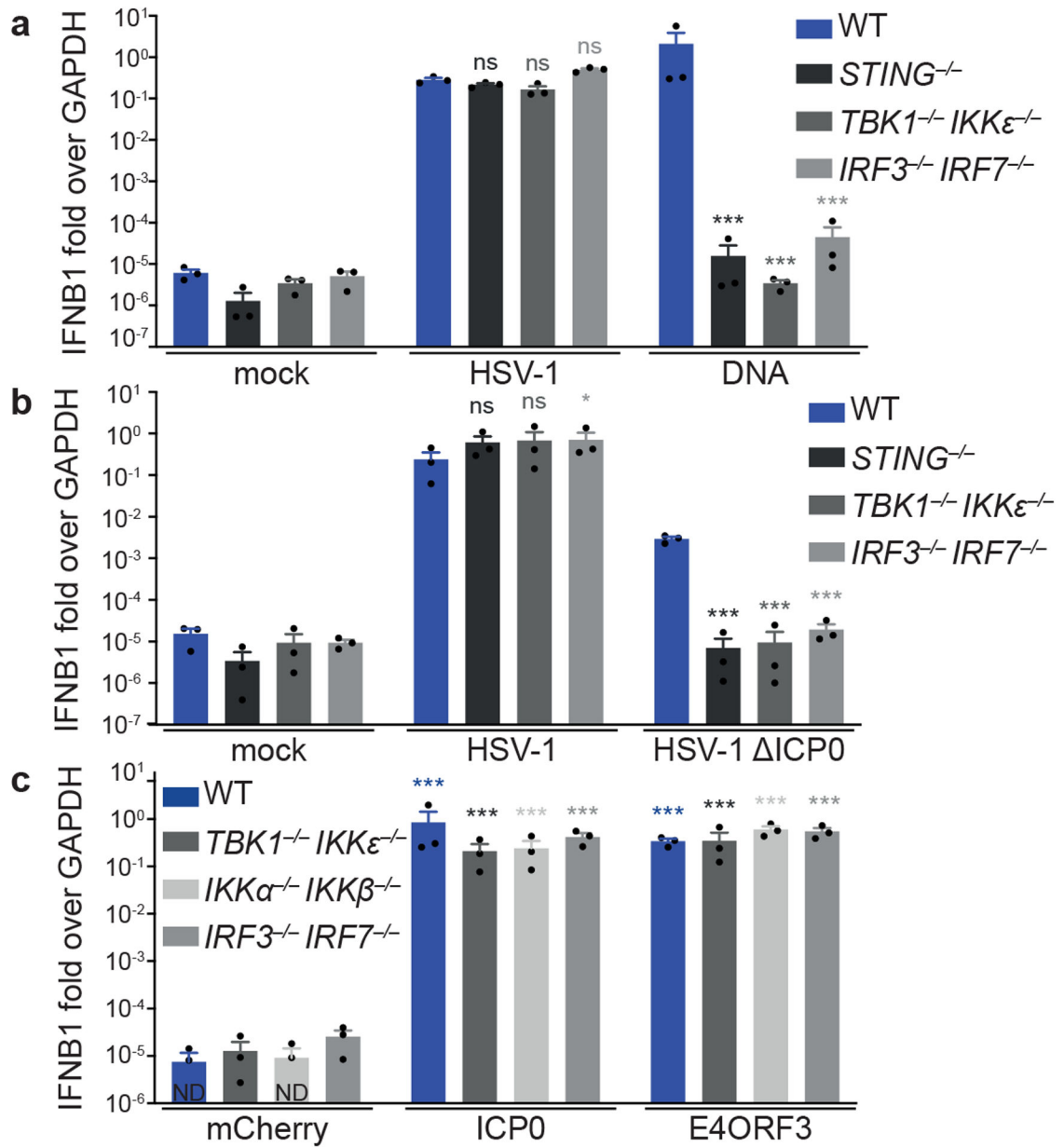
Figure 1: Virulence factor-triggered immune sensing

(a, b) BLaER1 monocytes were infected with HSV-1 at MOI=1 for 24h or transfected with DNA for 3h.

(c) BLaER1 monocytes expressing doxycycline-inducible virulence factors were stimulated with doxycycline for 24h.

Gene-expression is depicted as mean + SEM of three independent experiments.* $p < 0.05$; *** $p < 0.001$; ns = not significantly different than WT/mCherry, tested by two-way ANOVA and Dunnett's post hoc test. ND = not detected. See Source Data for exact p values.
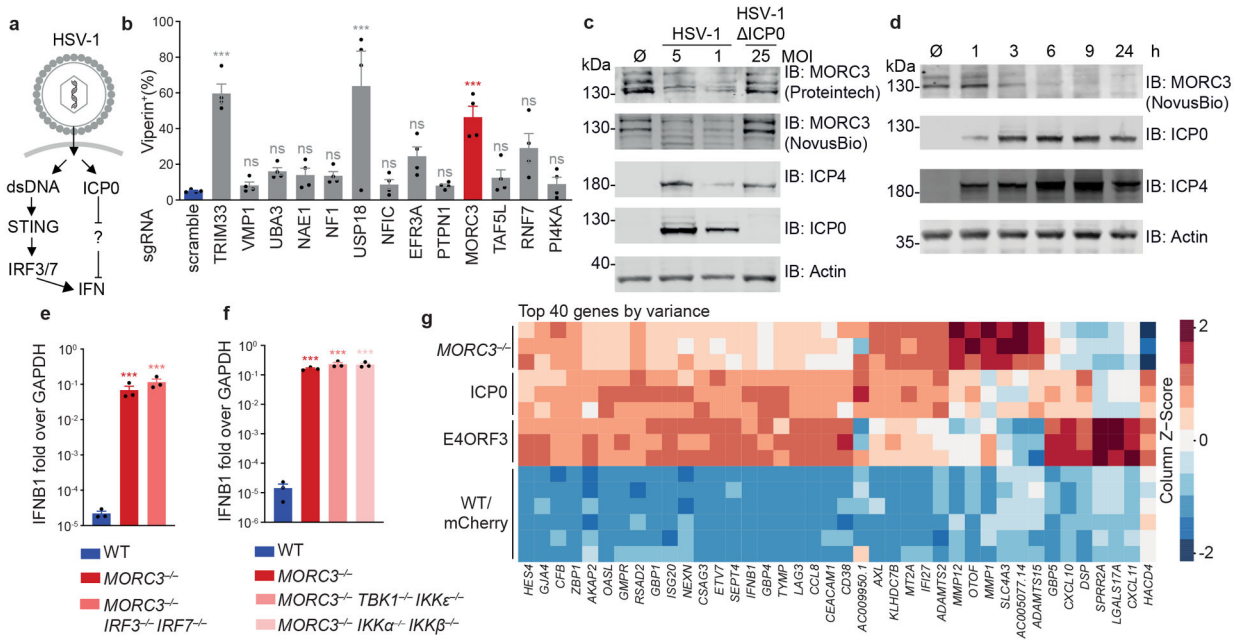
Figure 2: MORC3 is a novel negative regulator of IFN

(a) Hypothesized mechanism in which ICP0 degrades a negative regulator of IFN.

(b) FACS-analysis of Cas9-BLaER1 cells expressing sgRNAs. Mean + SEM of n=4 independent experiments.

(c) *IFNAR1⁻/⁻IFNAR2⁻/⁻STING⁻/⁻SP100⁻/⁻* BLaER1 monocytes (lacking factors that restrict ΔICP0 HSV-1) were infected with HSV-1 for 3h. One representative immunoblot of two is shown.

(d) *STING⁻/⁻* BLaER1 monocytes were infected with HSV-1 at MOI=5. One representative immunoblot of two is shown.

(e, f) Gene expression of BLaER1 monocytes is shown as mean + SEM of n=3 independent experiments from one representative clone of two (multiple KOs) or one clone (WT and *MORC3⁻/⁻*).

(g) Heatmap analysis (column normalized) of gene expression in BLaER1 monocytes as detected by RNA-seq in three independent experiments.

*** p < 0.001; ** p < 0.01; ns = not significantly different than scramble sgRNA or WT, tested by one-way or two-way ANOVA and Dunnett's post hoc test. See Source Data for exact p values.
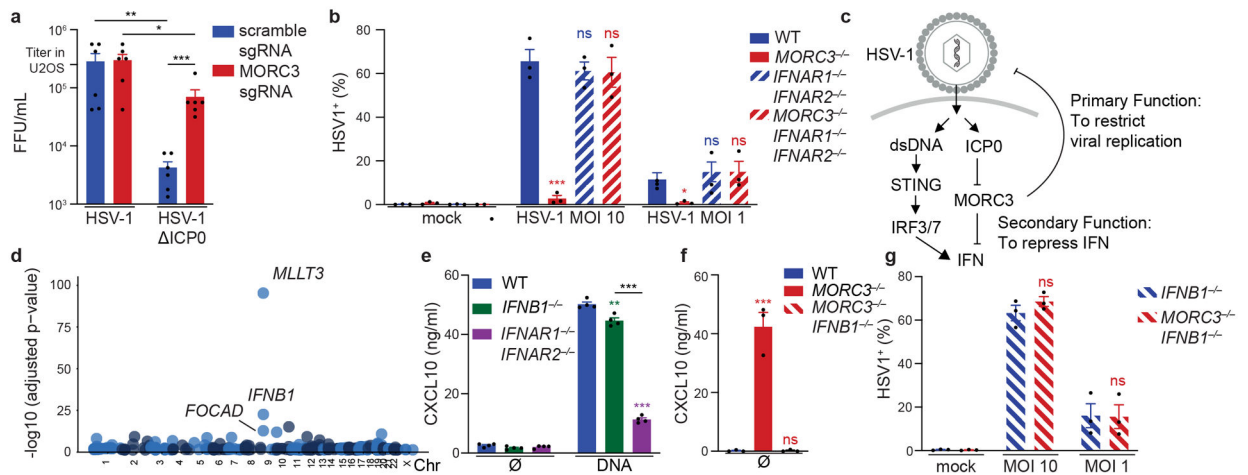
Figure 3: Locus-specific repression of *IFNB1* by MORC3 allows self-guarding

(a) The titer of HSV-1 stocks at 2.5×10^5 U2OS-FFU/ml was determined on HCT116-Cas9 cells expressing sgRNAs. Mean + SEM of n=6 independent experiments.

(b) BLaER1 monocytes were infected with HSV-1 for 6h and analyzed by flow cytometry. Mean + SEM of n=3 independent experiments.

(c) Two proposed functions of MORC3 that allow self-guarding.

(d) Upregulated genes in RNA-seq of *MORC3$^{-/-}$ IFNAR1$^{-/-}$ IFNAR2$^{-/-}$* vs *IFNAR1$^{-/-}$IFNAR2$^{-/-}$* BLaER1 monocytes are shown according to their genomic location.

(e, f) CXCL10 secretion of BLaER1 monocytes stimulated with DNA for 12h or left untreated. Mean + SEM of four (e) or three (f) independent experiments.

(g) BLaER1 monocytes were infected with HSV-1 for 6h and analyzed by flow cytometry. Mean + SEM of n=3 independent experiments are depicted. This data is from the same experiments as shown in (b).

$* p < 0.05$; $** p < 0.01$; $*** p < 0.001$; ns = not significantly different than WT (unless otherwise indicated), tested by paired, two-sided t-test (a) or by two-way ANOVA and Bonferroni's or Dunnett's post hoc test (b, e-g). See Source Data for exact p values.
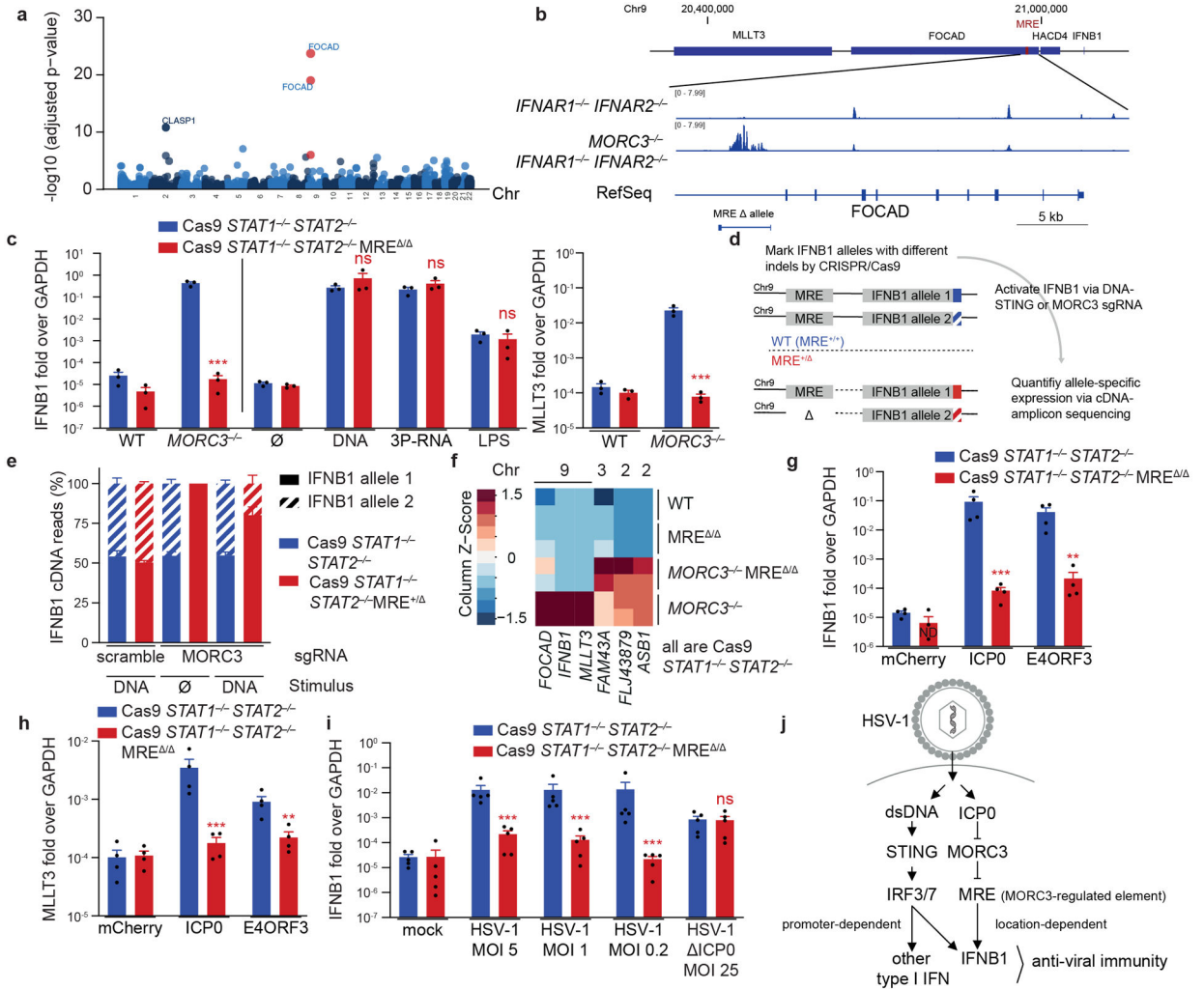
Figure 4: A MORC3-regulated DNA element explains positional *IFNB1* activation

(a) Non-promoter-associated ATAC-seq peaks of increased accessibility in *MORC3*^{-/-} *IFNAR1*^{-/-}*IFNAR2*^{-/-} vs *IFNAR1*^{-/-}*IFNAR2*^{-/-} BLaER1 monocytes. Peaks overlapping with the MRE are highlighted in red.

(b) A MORC3-regulated DNA element located in an intron of *FOCAD*. Sum of normalized ATAC-seq reads from three independent experiments is depicted. Alignment of sequencing reads indicating a MRE allele are indicated.

(c) BLaER1 monocytes were stimulated with PAMPs for 3h or left untreated. Gene expression is shown as mean + SEM of three independent experiments.

(d, e) Allele-specific *IFNB1* expression was determined in BLaER1 monocytes expressing sgRNAs and/or stimulated with DNA for 3h. Data is depicted as mean + SEM of three independent clones (harboring different *IFNB1* indels) as the average from three experiments.

(f) Heatmap analysis (column normalized) of gene expression in BLaER1 monocytes as detected by RNA-seq in two independent experiments. The six high-confidence MORC3-regulated genes (de-repressed in *MORC3*^{-/-} *IFNAR1*^{-/-}*IFNAR2*^{-/-}, *MORC3*^{-/-} *IFNB1*^{-/-} and *MORC3*^{-/-} *STAT1*^{-/-}*STAT2*^{-/-} Cas9) cells are depicted.

(g, h) BLaER1 monocytes expressing doxycycline-inducible virulence factors were stimulated with doxycycline for 24h. Gene expression is shown as mean + SEM of four independent experiments.

(i) BLaER1 were infected with HSV-1 at indicated MOI for 4–5h. Gene expression is shown as mean + SEM of five independent experiments.

(j) Overview of the self-guarded MORC3 pathway that detects virulence factors from DNA viruses via genomic location-dependent de-repression of *IFNB1*.

** $p < 0.01$; *** $p < 0.001$; ns = not significantly different than WT tested by two-way ANOVA and Bonferroni's post hoc test. See Source Data for exact p values.